NASA CR-72121

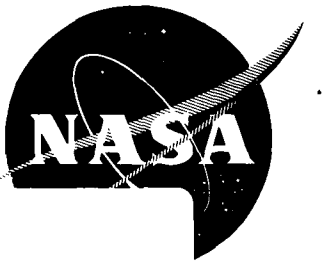

FINAL REPORT
VOLUME I

OSCILLATIONS IN TWO-COMPONENT TWO-PHASE FLOW

by

A. H. Stenning and T. N. Veziroglu

prepared for

NATIONAL AERONAUTICS AND SPACE ADMINISTRATION
NASA GRANT NsG - 424

Mechanical Engineering Department
University of Miami
Coral Gables, Florida

Requests for copies of this report should be referred to

National Aeronautics and Space Administration
Office of Scientific and Technical Information
Attention: AFSS-A
Washington, D.C. 20546

NASA CR-72121

FINAL REPORT

VOLUME I

OSCILLATIONS IN TWO-COMPONENT TWO-PHASE FLOW

by

A. H. Stenning and T. N. Veziroglu

prepared for

NATIONAL AERONAUTICS AND SPACE ADMINISTRATION

February 1967

NASA GRANT NsG-424

Technical Management
NASA Lewis Research Center
Cleveland, Ohio

James J. Watt

MECHANICAL ENGINEERING DEPARTMENT
UNIVERSITY OF MIAMI
CORAL GABLES, FLORIDA

OSCILLATIONS IN TWO-COMPONENT TWO-PHASE FLOW

by

A. H. Stenning and T. N. Veziroglu

ABSTRACT

The stability of two-component two-phase flow has been investigated both analytically and experimentally. In analytical work, solutions for three different systems of growing complexity have been obtained. The theoretical results are presented as stability maps, showing the relationships between density changes, dynamic pressure, pressure drops, mixer length, and inlet and exit ducting lengths at the boundaries of stable and unstable regions of operation. In experimental work, air and water were used as two-phase mixture components in a downward flow geometry for several ducting configurations. Agreement has been obtained between theoretical and experimental results.

CONTENTS

1. SUMMARY

2. INTRODUCTION

3. THEORETICAL STUDIES

- 3.1. Case I
- 3.2. Case II
  - 3.2.1. Mass continuity
  - 3.2.2. Volume continuity
  - 3.2.3. Pressure drop
  - 3.2.4. Analog computation
  - 3.2.5. Computer results
  - 3.2.6. Conclusions
- 3.3. Case III
  - 3.3.1. Mass continuity
  - 3.3.2. Volume continuity
  - 3.3.3. Pressure drop
  - 3.3.4. Analog computation
  - 3.3.5. Computer results
  - 3.3.6. Conclusions

4. EXPERIMENTAL STUDIES

- 4.1. Apparatus
- 4.2. Orifice Characteristics Experiments
  - 4.2.1. Experimental procedure
  - 4.2.2. Experimental results
- 4.3. Slip Ratio Experiments
  - 4.3.1. Experimental procedure
  - 4.3.2. Experimental results
- 4.4. Instability Experiments
  - 4.4.1. Experimental procedure
  - 4.4.2. Experimental results

5. COMPARISON OF EXPERIMENTS WITH THEORY

6. CONCLUSIONS

ACKNOWLEDGEMENTS

REFERENCES

NOMENCLATURE

FIGURES

were selected. Air and water were chosen as the two-phase components. Two sets of steady-state experiments were carried out to verify the relationships assumed to define the two-phase flow orifice characteristics and the slip ratio employed in the analysis. Also, stability experiments have been carried out to determine the boundaries of flow oscillations for several ducting configurations. Over a wide range of the variables the density ratio for instability is predicted within 30 percent. The frequency of the oscillations is predicted within 7 per cent for the case where theoretical values are available.

Parts of this final report have been reported earlier in the form of status reports and papers [1 thru 6].*

* Numbers in square brackets designate References at the end of the report, on page 52.

OSCILLATIONS IN TWO-COMPONENT TWO-PHASE FLOW

by

A. H. Stenning and T. N. Veziroglu
University of Miami

1. SUMMARY

Two-phase flows can conveniently be divided into two classes with respect to the liquid and gas components: (a) two-component two-phase flows in which the components are of different substances and the two-phase mixture is obtained by mixing (usually adiabatic), and (b) one-component two-phase flows in which both components are of the same substance and the two-phase mixture is obtained by boiling a liquid. Accordingly the investigation of two-phase flow instabilities has been divided into two parts, and the present report gives an account of the work on the two-component two-phase flow instabilities.*

The stability of two-component two-phase flow has been studied both analytically and experimentally. In analytical work, a step-by-step approach has been followed starting with an exact solution of the governing differential equations for a very simple flow system. For more complex system, solutions have been obtained using analog computers. The theoretical results are presented as stability maps, showing the relationships between various dimensionless parameters at the boundaries of stable and unstable regions of operation.

In experimental work, single-channel system geometries similar to those used in the analytical study

---

* The complementary report is "Flow Oscillations in Forced Convection Boiling", NASA GRANT NsG-424, Final Report - Volume II, NASA CR-72122, February, 1967.

2. INTRODUCTION

Oscillations in two-phase flow, with and without boiling, have been observed in many systems in which a gas is mixed with a liquid, or a liquid is vaporized [7]. Systems displaying these oscillations are frequently too complex to permit comparison of the observed behavior with theory, and in consequence a great deal of experimental information has been gathered which can not be correlated.

The objective of this investigation was to study two-phase flow oscillations in a simple flow configuration (a single channel flow geometry) and under most advantageous experimental conditions. A two-component two-phase flow system offers some experimental advantages over a one-component two-phase flow system with boiling. The flow rate of each phase can be controlled and measured independently, the uncertainties of boiling heat transfer are avoided, and the experiments can be carried out under isothermal conditions. The single channel system considered, in general, consists of some inlet ducting, an inlet valve, a mixer, some exit ducting and an exit orifice. The liquid component flows through the inlet ducting and inlet valve into the mixer where the gas component is introduced at a constant rate to produce a two-phase mixture. Then the mixture flows through the exit ducting and the exit orifice.

The type of two-component, two-phase flow instability investigated consists of oscillations in the flow rate of the liquid component which produce fluctuations in the density of the mixture. The oscillations are caused by the sensitivity of the exit orifice volume flow characteristic to mixture density. For a given pressure drop across the exit orifice, the volume flow rate through the orifice is inversely proportional to some power of the mixture density (the square root of the density for a single-phase fluid). Hence, if a small increase in mixture density occurs at the exit orifice, the volume flow rate through the system is reduced. An excess of gas accumulates in the mixer, and after a time equal to the residence time of a particle in the system, a portion of the mixture with reduced density appears at the orifice. This causes an increase in volume flow rate through the system, so that the next portion of liquid passing through the mixer picks up less gas than the preceding one and arrives at the orifice with high mixture density. Thus, if a critical average density ratio from inlet to exit is exceeded, the system is unstable for perturbations from the steady state and oscillations are set up. By increasing the inlet-valve pressure drop, it is found that the system can be stabilized and returned to a steady-state.

The two-component two-phase flow oscillations studied herein are of the same nature as Type II (density-wave) oscillations encountered in boiling flows.

3. THEORETICAL STUDIES

With the exception of the most simple case (a mixer with an exit restriction) it was not possible to integrate and obtain analytical solutions of the differential equations describing the dynamics of systems containing two-phase flow. Hence, small perturbation and analog methods were used in studying two-phase flow and the conditions at the onset of instability. A step by step analysis approach was employed. Three cases are presented in order of increasing complexity.

The system to be considered is a single channel flow system, and the simplest case consists of a mixer and an exit orifice. In the intermediate case, an inlet valve and some exit ducting are added before and after the mixer respectively. In the final case, the system additionally includes some inlet ducting, Overall pressure drop across the system was assumed to remain constant in all the cases. The flow was assumed to be homogeneous, and gravitational and slip effects neglected. According to Meyer and Rose [8], neglecting the slip (i.e., assuming the liquid and vapor velocities are equal) leads to somewhat pessimistic estimates of system stability and is therefore on the conservative side.

The simplest case will be considered first because it has an exact analytical solution. This solution will be helpful in checking the accuracy of the approximations employed in the more general cases.

3.1. Case I

Fig. 1 shows the simplest two-phase flow system considered. Liquid flows into a mixer where it mixes with a gas seeping uniformly through the wall. The two-component two-phase mixture flows out of an exit orifice. It will be assumed that the pressure changes within the mixer are small so that the gas density can be taken to remain constant in the mixer. For the analysis of the flow a method used by Wallis and Heasley [9] will be employed.

Let U^* be the mean flow velocity at a given cross-section of the mixer of length L and cross-sectional area A. Let subscripts i and e refer to the inlet and exit conditions. Then the flow velocity at a distance x from the mixer inlet will be,

$$U = U_i + \frac{Q}{A}\frac{x}{L} \quad \text{.....................................(1)}$$

where Q is the volume flow rate of the gas into the mixer. Hence the flow velocity at the mixer exit will be,

$$U_e = U_i + \frac{Q}{A} \quad \text{.....................................(2)}$$

If x is the distance covered by a "two-phase" particle, then,

$$U = \frac{dx}{dt} \quad \text{...(3)}$$

---

* A nomenclature is included at the end of the report on page 54.

From equations (1) and (3),

$$\frac{dx}{dt} - \frac{Q}{AL} x = U_i \quad \ldots\ldots\ldots\ldots\ldots\ldots\ldots\ldots (4)$$

The inlet velocity U_i will be a function of time when the instability starts. Hence, in order to solve equation (4) for the general case, let us multiply both side by $\exp\ (- \frac{Q}{AL}\ t)$,

$$\exp\ (- \frac{Q}{AL}\ t)\ \frac{dx}{dt} - \exp(- \frac{Q}{AL}\ t)\ \frac{Q}{AL}\ x = \exp(- \frac{Q}{AL}\ t) U_i$$

or,

$$\frac{d}{dt}\ \{x \exp\ (- \Phi t)\ \} = \exp\ (- \Phi t) U_i \quad \ldots\ldots\ldots\ldots (5)$$

where $$\Phi = \frac{Q}{AL} \quad \ldots\ldots\ldots\ldots\ldots\ldots\ldots\ldots\ldots\ldots (6)$$

The symbol Φ is the time rate of gas volume introduction per unit volume of the mixer and has dimension of time^{-1}. Integrating equation (5) with respect to time and solving for x,

$$x = \exp\ (\Phi t) \int_o^t \exp\ (- \Phi t')\ U_i\ dt' \quad \ldots\ldots\ldots\ldots (7)$$

where the time is taken as zero when the particle is at the mixer inlet.

From continuity considerations, the relationship between the mixture density ρ, velocity U, distance x from the inlet, and time t, for a constant cross sectional area mixer, will be given by

$$\frac{\partial \rho}{\partial t} + \frac{\partial \rho U}{\partial x} = \frac{Q \rho_g}{AL} \quad \ldots\ldots\ldots\ldots\ldots\ldots\ldots\ldots (8)$$

where ρ_g is the gas density.

Rearranging equation (8),

$$\frac{D\rho}{Dt} + \rho \frac{\partial U}{\partial x} = \frac{Q\rho_g}{AL} \quad \ldots\ldots\ldots\ldots\ldots\ldots\ldots\ldots (9)$$

Differentiating equation (1) with respect to x,

$$\frac{\partial U}{\partial x} = \frac{Q}{AL} = \Phi \quad \ldots\ldots\ldots\ldots\ldots\ldots\ldots\ldots (10)$$

Substituting equation (10) in equation (9), and rearranging,

$$\frac{D\rho}{Dt} + \Phi \ (\rho - \rho_g) = 0 \quad \ldots\ldots\ldots\ldots\ldots\ldots\ldots\ldots (11)$$

Integrating equation (11), the relationship between the density of a "two-phase" particle and time, as the particle moves along the mixer, becomes,

$$\rho = C \ e^{-\Phi t} + \rho_g \quad \ldots\ldots\ldots\ldots\ldots\ldots\ldots\ldots (12)$$

where C is a constant.

Using the boundary condition that $\rho = \rho_i$ when $t = o$, together with equation (12), results in,

$$C = \rho_i - \rho_g \quad \ldots\ldots\ldots\ldots\ldots\ldots\ldots\ldots (13)$$

Substituting equation (13) in (12),

$$\rho = (\rho_i - \rho_g) \ e^{-\Phi t} + \rho_g \quad \ldots\ldots\ldots\ldots\ldots\ldots\ldots\ldots (14)$$

If t_r is the residence time of a particle in the mixer, then the exit density becomes,

$$\rho_e = (\rho_i - \rho_g)\, e^{-\Phi t_r} + \rho_g \quad \ldots\ldots\ldots\ldots\ldots\ldots (15)$$

Here, it may be noted that the inlet density is equal to the liquid density.

Assuming that single phase orifice relationship holds for two-phase flows, and that the pressure drop across the system is constant with a negligible pressure drop in the mixer, the flow velocity at the mixer exit can be expressed as,

$$U_e = K\, \rho_e^{-1/2} \quad \ldots\ldots\ldots\ldots\ldots\ldots\ldots\ldots (16)$$

where K is a constant for a given orifice and a given pressure drop.

Consider small perturbations in exit velocity and exit density. Differentiating equation (16) and rearranging, one obtains,

$$\frac{d\rho_e}{2\rho_e} + \frac{dU_e}{U_e} = 0 \quad \ldots\ldots\ldots\ldots\ldots\ldots\ldots\ldots (17)$$

For small perturbations in U, assuming that the gas flow rate into the mixer Q remains constant, equation (2) yields

$$dU_e = dU_i \quad \ldots\ldots\ldots\ldots\ldots\ldots\ldots\ldots (18)$$

Substituting equation (18) in (17),

$$\frac{d\rho_e}{2\rho_e} + \frac{dU_i}{u_e} = 0 \quad \ldots\ldots\ldots\ldots\ldots\ldots\ldots\ldots (19)$$

Differentiating and rearranging equation (15), the following expression for the first term of the above equation can be obtained,

$$\frac{d\rho_e}{\rho_e} = - \frac{\rho_e - \rho_g}{\rho_e} \Phi \, dt_r \quad \ldots\ldots\ldots\ldots\ldots\ldots (20)$$

Substituting equations (15) and (20) in (19),

$$- \frac{\Phi dt_r}{2 + \frac{2\rho_g}{\rho_i - \rho_g} e^{\Phi t_r}} + \frac{dU_i}{U_e} = 0 \quad \ldots\ldots\ldots\ldots\ldots (21)$$

The relationship between the inlet and exit densities and velocities, from continuity of mass flow rates, becomes,

$$A \, U_i \, \rho_i + Q \, \rho_g = A \, U_e \, \rho_e \quad \ldots\ldots\ldots\ldots\ldots\ldots (22)$$

Solving equation (22) for U_e and substituting equations (6) and (15),

$$U_e = \frac{U_i \, \rho_i + \Phi L \, \rho_g}{(\rho_i - \rho_g) \, e^{-\Phi t_r} + \rho_g} \quad \ldots\ldots\ldots\ldots\ldots\ldots (23)$$

Substituting equation (23) in (21), one obtains,

$$- \frac{\Phi(\rho_i - \rho_g) e^{-\Phi t_r} \, dt_r}{2(\rho_i - \rho_g) e^{-\Phi t_r} + 2\rho_g} + \frac{(\rho_i - \rho_g) e^{-\Phi t_r} + \rho_g \; dU_i}{U_i \, \rho_i + \Phi L \, \rho_g} = 0$$

$$\ldots\ldots\ldots\ldots\ldots\ldots (24)$$

Consider small oscillations in the inlet velocity given by the expression,

$$U_i = U_{io} + \epsilon e^{i\omega t} \quad \ldots\ldots\ldots\ldots\ldots\ldots\ldots (25)$$

where U_{io} is the mean inlet velocity, ϵ amplitude of the small velocity oscillations and ω the frequency of the oscillations. It will be noticed that when the particle considered above starts its journey at the mixer inlet its velocity is U_{io}. In other words at the time zero, the assumed velocity oscillations pass through their mean value. This choice results in some simplifications to the equations, though it is not a necessary condition for analyzing the problem.

Substituting equation (25) in (7),

$$x = e^{\Phi t} \int_o^t e^{-\Phi t'} \{U_{io} + \epsilon e^{i\omega t'}\} dt' \quad \ldots\ldots\ldots (26)$$

Integrating equation (26) between the limits,

$$x = \frac{U_{io}}{\Phi} \{e^{\Phi t} - 1\} + \frac{\epsilon e^{i\omega t}}{i\omega - \Phi} \{1 - e^{(\Phi - i\omega)t}\} \quad \ldots\ldots (27)$$

If $t = t_r$, then x should be equal to L. Hence, from equation (27),

$$L = \frac{U_{io}}{\Phi} \{e^{\Phi t_r} - 1\} + \frac{\epsilon e^{i\omega t_r}}{i\omega - \Phi} \{1 - e^{(\Phi - i\omega)t_r}\} \quad \ldots\ldots\ldots\ldots (28)$$

Assume that the residence time t_r has two components, one a constant residence time T_r equal to the residence time of a particle at steady state with an inlet velocity of U_{io}, and the other δt_r a small change in residence time due to superimposed inlet velocity oscillations i.e.,

$$t_r = T_r + \delta t_r \quad \ldots\ldots\ldots\ldots\ldots\ldots\ldots\ldots (29)$$

Substituting equation (29) in (28),

$$L = \frac{U_{io}}{\Phi} \{e^{\Phi T_r} e^{\Phi \delta t_r} - 1\}$$

$$+ \frac{\epsilon e^{i\omega T_r} e^{i\omega \delta t_r}}{i\omega - \Phi} \{1 - e^{(\Phi - i\omega)T_r} e^{(\Phi - i\omega)\delta t_r}\}$$

.....(30)

If there are no oscillations, the equation (30) reduces to,

$$L = \frac{U_{io}}{\Phi} \{e^{\Phi T_r} - 1\} \quad \text{.....(31)}$$

Since small oscillations are being considered,

$$e^{\Phi \delta t_r} \approx 1 + \Phi \delta t_r \ , \ e^{i\omega \delta t_r} \approx 1 + i\omega \delta t_r \quad \text{.....(32)}$$

Substituting equations (31) and (32) in (30), and solving for δt_r, one obtains,

$$\delta t_r = - \frac{\epsilon e^{i\omega T_r} \{1 - e^{(\Phi - i\omega)T_r}\}}{(i\omega - \Phi) U_{io} e^{\Phi T_r} + \epsilon e^{i\omega T_r} \{i\omega - (\Phi - \omega) e^{(\Phi - \omega)T_r}\}}$$

.....(33)

From equation (25), the change in inlet velocity from its mean value during the residence of a particle in the mixer becomes,

$$\delta U_i = \epsilon e^{i\omega T_r} \quad \text{.....(34)}$$

For small oscillations (i.e., at the onset of oscillations) $\delta t_r \rightarrow dt_r$ and $\delta U_i \rightarrow dU_i$. Because of this equivalence, substituting equations (25), (33) and (34) in (24), and allowing the amplititude of the oscillations to vanish, one obtains,

$$\frac{\Phi\{1 - e^{(\Phi - i\omega) T_r}\}}{2 \{i\omega - \Phi\}} + \frac{U_{io}\{(\rho_i - \rho_g) e^{-\Phi T_r} + \rho_g\}^2}{(\rho_i U_{io} + \Phi L \rho_g) (\rho_i - \rho_g) e^{-2\Phi T_r}} = 0.$$

.....(35)

This is then the equation which must be satisfied at the

onset of two-component two-phase flow instability if it exists. The equation (35) can be simplified somewhat. Densities of gases are very much smaller than those of liquids, i.e., $\rho_g << \rho_i$. In addition, experiments indicate that exit densities for the instability-onset conditions are much greater than those of gases, or, for onset conditions $\rho_g << \rho_e$. From these two inequalities it follows that for the onset conditions the liquid mass flow rates must be much greater than the gas mass flow rates. In other words, $A\rho_i U_i >> Q\rho_g$ or $\rho_i U_i >> \Phi L\rho_g$. Consequently, neglecting ρ_g with respect to ρ_i and ρ_e, and $\Phi L\rho_g$ with respect to $U_{io}\rho_i$ in equation (35), one obtains,

$$\frac{\Phi\{1 - e^{(\Phi - i\omega)\ T_r}\}}{2\ \{i\omega - \Phi\}} + 1 = 0 \quad \ldots\ldots\ldots\ldots\ldots\ldots (36)$$

Substituting the trigonometric expression of the exponential function in equation (36), and rearranging,

$$2\ i\omega - \Phi = \Phi\ e^{\Phi T_r}\ \{\cos(\omega\ T_r) - i\ \sin(\omega\ T_r)\ \} \quad \ldots\ldots\ldots\ldots (37)$$

For equation (37) to hold, the real and imaginary parts must vanish, i.e.,

$$-\ \Phi = \Phi\ e^{\Phi T_r} \cos\ (\omega\ T_r) \quad \ldots\ldots\ldots\ldots\ldots\ldots (38)$$

$$2\omega = -\ \Phi\ e^{\Phi T_r} \sin(\omega\ T_r) \quad \ldots\ldots\ldots\ldots\ldots\ldots (39)$$

or

$$1 = -\ e^{\Phi T_r} \cos\ (\omega T_r) \quad \ldots\ldots\ldots\ldots\ldots\ldots (40)$$

$$2\omega\ T_r = -\Phi T_r e^{\Phi T_r} \sin\ (\omega T_r) \quad \ldots\ldots\ldots\ldots\ldots\ldots (41)$$

Solving equations (40) and (41) by trial and error, the values of ΦT_r and ωT_r at the onset of instability become,

$$\Phi T_r = 1.694 \quad \ldots\ldots (42)$$

and

$$\omega T_r = 4.527 \quad \ldots\ldots (43)$$

Equation (42) gives the relationship between the residence time (T_r) and the time rate of gas volume introduction per unit volume of mixer (Φ), and equation (43) gives the relationship between the residence time and the frequency of the oscillations (ω) at the onset of instability. Fig. 2 is a plot of equation (42). An inspection shows that the region within the hyperbola corresponds to unstable operation and the region between the hyperbola and the reference axis corresponds to stable operation. From equations (42) and (43) the following relationship between Φ and ω can be obtained,

$$\frac{\omega}{\Phi} = 2.67 \quad \ldots\ldots (44)$$

Using the above calculated values, it is possible to find an expression for the overall density ratio (inlet density divided by exit density) at the onset of instability. The overall density ratio, r, by definition is given by,

$$r = \frac{\rho_i}{\rho_e} \quad \ldots\ldots (45)$$

Substituting equation (15) in (45),

$$r = \frac{\rho_i}{(\rho_i - \rho_g)\ e^{-\Phi T_r} + \rho_g} \quad \ldots\ldots (46)$$

Substituting equation (42) in (46),

$$r = 5.44 \frac{\rho_i}{\rho_i + 4.44\ \rho_g} \quad \ldots\ldots\ldots\ldots\ldots\ldots\ldots\ldots (47)$$

Since, in general, $\rho_i >> \rho_g$, equation (47) reduces to,

$$r \approx 5.44 \quad \ldots\ldots\ldots\ldots\ldots\ldots\ldots\ldots\ldots\ldots\ldots\ldots (48)$$

For overall density ratios below 5.44, the system is stable, and for overall density ratios above 5.44 unstable.

From the above analysis of a simple two-component two-phase flow system (consisting of a mixer and an exit orifice) having a constant overall pressure drop and a uniform rate of gas injection, the following conclusions are arrived at:

a. In the simple two-phase flow system considered, it was found that instabilities characterized by periodic flow velocity and mixture density changes, take place.

b. The system is stable for overall density ratios below about 5.44 and unstable for overall density ratios above it.

c. In addition to the overall density ratio criteria, there are simple relationships between residence time, frequency of oscillations and time rate of gas volume injection per unit volume of mixer at the onset of instability. These are given by equations (42), (43) and (44).

3.2. Case II

The system to be considered has more components than Case I, as shown in Fig. 3. It consists of an inlet valve, a mixer, some exit ducting and an exit orifice. Liquid flows through the inlet valve into the mixer in which a gas is injected into the liquid at a constant rate. The mixture of liquid and gas then flows out through the exit ducting and exit orifice.

Since the differential equations describing the two-component two-phase flow in this system could not be directly integrated, a lumped parameter analog computer program will be used to study the flow. As seen in Fig. 3, the system is divided into several lumps, and the equations describing the flow are written for each lump.

3.2.1. Mass Continuity

For a mixer lump, as shown in Fig. 4, the mass continuity equation may be written as,

$$\rho_n (UA)_n + \rho_g Q - \rho_{n+1} (UA)_{n+1} = \frac{Vn}{2} \cdot \frac{d}{dt} \{\rho_n + \rho_{n+1}\} \ldots\ldots \quad (49)$$

where V_n is the volume of the lump and Q is the volume flow rate of gas into the lump. The average density is assumed to be the arithmetic mean of the inlet and outlet densities.

Dividing both sides of equation (49) by $\rho_{es} (UA)_{es}$, where ρ_{es} is the mixture density leaving the exit ducting at steady state and $(UA)_{es}$ is the volume flow rate leaving the exit ducting at steady state, one obtains,

$$r_n u_n + r_g q - r_{n+1} u_{n+1} = \frac{V_n}{2(UA)_{es}} \cdot \frac{d}{dt} (r_n + r_{n+1}) \quad \ldots\ldots (50)$$

where

$$r_n = \frac{\rho_n}{\rho_{es}} , \quad r_{n+1} = \frac{\rho_{n+1}}{\rho_{es}} , \quad r_g = \frac{\rho_q}{\rho_{es}}$$

$$u_n = \frac{(UA)_n}{(UA)_{es}} , \quad u_{n+1} = \frac{(UA)_{n+1}}{(UA)_{es}} , \quad q = \frac{Q}{(UA)_{es}}$$

Let

$$T = \frac{2(UA)_{es}}{V_n} t \quad \ldots\ldots (51)$$

Substituting equation (51) in (50),

$$r_n u_n + r_g q - r_{n+1} u_{n+1} = \frac{d}{dT} (r_n + r_{n+1}) \quad \ldots\ldots (52)$$

For an exit ducting lump, equation (52) reduces to,

$$r_n u_n - r_{n+1} u_{n+1} = \frac{d}{dT} (r_n + r_{n+1}) \quad \ldots\ldots (53)$$

Since then $q = o$.

At steady state $r_e = 1$ and $u_e = 1$. Consequently, at steady state, for mixer lump number n,

$$r_n u_n + (m - n + 1) r_g q = 1 \quad \ldots\ldots (54)$$

where m is the number of mixer lumps.

And for an exit ducting lump,

$$r_n u_n = 1 \quad \ldots\ldots (55)$$

3.2.2. Volume continuity

Consider a mixer lump. If the compressibility effect is neglected (i.e. assuming negligible pressure changes),

the mixture volume flow rate out of the lump is greater than the volume flow rate into the lump by the amount of gas volume flow rate into the lump. i.e.,

$$(UA)_{n+1} - (UA)_n = Q \quad \ldots\ldots(56)$$

Dividing both sides by $(UA)_{es}$,

$$u_{n+1} - u_n = q \quad \ldots\ldots(57)$$

At steady state the difference between dimensionless exit and inlet flow velocities, from equation (57), becomes,

$$u_{es} - u_{is} = mq \quad \ldots\ldots(58)$$

or

$$u_{is} = 1 - mq \quad \ldots\ldots(59)$$

since $u_{es} = 1$.

From equation (54), the overall density ratio for steady state, r_{is}, is given by,

$$r_{is} = \frac{1 - mr_g\, q}{u_{is}} \quad \ldots\ldots(60)$$

Substituting equation (59) in (60)

$$r_{is} = \frac{1 - mr_g\, q}{1 - mq} \quad \ldots\ldots(61)$$

3.2.3. Pressure drop

The overall pressure drop ΔP_t is the sum of inlet valve, exit orifice, mixer and exit ducting pressure drops. For the inlet valve,

$$\Delta P_i = K_i \rho_i U_i^2 \quad \ldots\ldots (62)$$

where K_i is a constant depending on the inlet valve opening.

For the exit orifice,

$$\Delta P_e = K_e \rho_e U_e^2 \quad \ldots\ldots (63)$$

assuming that a relationship of this type can be used for two-phase flow. K_e in equation (63) is the exit orifice constant.

For the mixer plus exit ducting,

$$\Delta P_{ie} = \Delta P_f + \Delta P_m + \Delta P_d \quad \ldots\ldots (64)$$

where ΔP_f = Frictional Pressure Drop, ΔP_m = Momentum pressure drop and ΔP_d = dynamic pressure drop associated with unsteady flow. For a constant cross sectional area system with an effective friction factor f,

$$\Delta P_f = \frac{4fL}{D} \left\{ \frac{\rho_i U_i^2}{4} + \frac{\rho_e U_e^2}{4} \right\} \quad \ldots\ldots (65)$$

and

$$\Delta P_m = \rho_e U_e^2 - \rho_i U_i^2 \quad \ldots\ldots (66)$$

Assuming for simplicity that all the inertia is lumped on the inlet side of the system,

$$\Delta P_d = \rho_i \left(\Sigma \frac{L}{A}\right) \frac{d}{dt} (UA)_i \quad \ldots\ldots (67)$$

where $\Sigma L/A$ is summed for all the ducting in the system. The total pressure drop is,

$$\Delta P_t = \Delta P_i + \Delta P_{ie} + \Delta P_e \quad \ldots\ldots (68)$$

or, substituting for the pressure components,

$$\Delta P_t = \rho_i U_i^2 \{K_i + \frac{fL}{D} - 1\} + \rho_e U_e^2 \{K_e + \frac{fL}{D} + 1\}$$

$$+ \rho_i \{\Sigma \frac{L}{A}\} \frac{d}{dt} (UA)_i \quad \ldots\ldots\ldots\ldots\ldots\ldots\ldots\ldots (69)$$

Normalizing the right hand side,

$$\Delta P_t = K_i' r_i u_i^2 + K_e' r_e u_e^2 + \rho_i (UA)_{es} (\Sigma \frac{L}{A}) \frac{du_i}{dt}$$

$$\ldots\ldots\ldots\ldots\ldots\ldots\ldots\ldots (70)$$

where K_i' and K_e' are new constants. The same expression is obtained for a system of varying cross-sectional area if its resistance is approximated in terms of inlet and exit conditions. At steady state equation (70) reduces to

$$\Delta P_t = \frac{K_i' (1 - m r_g q)^2}{r_i} + K_e' \quad \ldots\ldots\ldots\ldots\ldots\ldots (71)$$

Dividing equation (70) by (71), and rearranging, one obtains,

$$\frac{du_i}{dT} = \frac{1}{\tau} \{1 - y \left(\frac{r_i u_i}{1 - m r_g q} \right)^2 - (1 - y) r_e u_e^2 \}$$

$$\ldots\ldots\ldots\ldots\ldots\ldots (72)$$

where,

$$T = \frac{2 (UA)_{es}}{V} t \quad \ldots\ldots\ldots\ldots\ldots\ldots\ldots\ldots (73)$$

$$\tau = \frac{2 \rho_i (UA)_{es}^2}{V \Delta P_t} \Sigma \frac{L}{A} \quad \ldots\ldots\ldots\ldots\ldots\ldots (74)$$

and

$$y = \frac{K_i' (1 - m r_g q)^2}{K_i' (1 - m r_g q)^2 + K_e' r_i} \quad \ldots\ldots\ldots\ldots\ldots\ldots (75)$$

In the above expressions, τ is a measure of dynamic pressure and is dimensionless, and y is the fraction of the total pressure drop attributable to the upstream ducting at steady state. For high density ratios y is nearly equal to $\Delta P_i / \Delta P_t$.

3.2.4 Analog computation

Equations (52), (53), (57), (61) and (72) can be programed on an analog computer to study the dynamics of two-component two-phase flow in the system under consideration. In studying the conditions at the onset of flow instabilities, the above equations can be simplified by considering the facts mentioned under the Chapter 3.1 Case I; i.e. in general $\rho_g << \rho_i$, and for instability onset conditions $\rho_g << \rho_e$ and the gas mass flow rate is very much smaller than the liquid mass flow rate. By making use of these facts, the equations can be reduced to,

$$r_n u_n - r_{n+1} u_{n+1} = \frac{d}{dT} (r_n + r_{n+1}) \quad \ldots\ldots (76)$$

$$u_{n+1} - u_n = q \quad \ldots\ldots \text{(for mixer lumps)} \quad \ldots\ldots (77)$$

$$r_{is} = \frac{1}{1 - mq} \quad \ldots\ldots (78)$$

$$\frac{du_i}{dT} = \frac{1}{\tau} \{1 - y(r_i u_i)^2 - (1-y) r_e u_e^2\} \quad \ldots\ldots (79)$$

The system was divided into a total of seven lumps, because of the number of computing elements available in the analog computer used - a Philbrick analog computer. The above equations were then programed on the computer.

The equations were not linearized. In operation, the system parameters were adjusted until the onset of instability was observed. This was determined by observing an oscilloscope image of density (or velocity) voltage at one of the stations, usually at the system exit, and adjusting the parameters until small oscillations were barely visible and were of constant amplitude. Then at this point the parameters were recorded.

3.2.5. Computer results

The analog computer results are plotted in Figs. 5 through 8 as the relationships between the parameters at onset of instability. Fig. 5 shows the relationship between the overall density ratio r_{is} and the system volume to mixer volume ratio V_t/V_m for no inlet pressure drop ($y = o$) and negligible inertia ($\tau = 0$). For these conditions with $V_t/V_m = 1$, an exact solution was obtained in section 3.1, which resulted in an overall density ratio of 5.44 at stability onset. The value obtained by means of the seven-lump analog computation was within 2 per cent of the exact solution. Another exact solution for the above conditions with $V_t/V_m = \infty$ has been obtained by Stenning [10]. The exact value of the overall density ratio at stability onset was shown to be 3. The analog computer solution exhibits correct behavior as the system volume to mixer volume ratio is increased, and when the

ratio is 7, the value of r_{is} at stability boundary is 3.10. These comparisons between the computer solutions and exact solutions show that the computer accuracy was satisfactory.

Fig. 6 shows the relationship between normalized time period of oscillations and the system volume to mixer volume ratio at stability onset for no inlet pressure drop and negligible inertia. The normalized time period decreases with increase in the volume ratio but at a decreasing rate as the volume ratio increases.

Fig. 7 shows the stability boundaries as curves of normalized inlet pressure drop y versus the inertia factor $(1/\tau)$ for a constant overall density ratio of 150 and for two mixer and exit ducting arrangements. The region above each curve is stable and below unstable. From a study of the figure it can be seen that the inlet pressure drop required to stabilize the flow increases - though at a decreasing rate - with increase in the inertia factor. Below a certain inertia factor, the system is completely stable. It can also be seen that decreasing the mixer length and/or increasing the exit ducting length has a beneficial effect on stability.

Fig. 8 shows the stability boundaries for various overall density ratios ranging from 10 to 500 when $V_t/V_m = 1$, i.e., when the system consists of an inlet valve, a mixer and an exit orifice but no exit ducting. It can be seen that at large values of the inertia factor $(1/\tau)$ the value of y for incipient instability is

independent of τ. As $1/\tau$ is reduced, a value is reached below which further reductions in $1/\tau$ have a marked stabilizing effect on the system.

In all cases, satisfactory damping could be obtained by increasing y above the value for zero damping by about 0.05. The onset of instability was quite abrupt, and small limit cycle oscillations rarely were observed. A very small reduction in y below the value for zero damping produced violent sustained oscillations in flow. A substantial increase in y then was required to eliminate the oscillations.

3.2.6. Conclusions

From the above analysis of a two-component two-phase flow system consisting of an inlet valve, a mixer, some exit ducting and an exit orifice, the following conclusions are arrived at:

a. The accuracy of the analog computer computations was satisfactory as evidenced by the comparison of the instability onset density ratios obtained by exact solutions and computer computations for the special cases.

b. Increase in total volume to mixer volume ratio decreases stability (Fig. 5) for a system with negligible inertia and low overall density ratios for instability onset.

c. Increase in total volume to mixer volume ratio decreases the normalized time period of oscillations at the stability boundary, for a system with negligible inertia and low overall density ratios for instability onset.

d. Increase in inlet pressure drop to overall pressure drop ratio increases stability.

e. Increase in system inertia increases stability.

f. Increase in overall density ratio decreases stability.

3.3. Case III

This is the most general case analyzed. As shown in Fig. 9, it consists of some inlet ducting, an inlet valve, a mixer, some exit ducting and an exit orifice. For analysis, the system was broken up into four lumps; one for the inlet ducting including the inlet valve, two equal lumps for the mixer section, and one for the exit ducting. The number of lumps was limited to four by the non-linear components available in the analog computer used, an EAI TR-48, but previous studies of lumping accuracy showed this number to be satisfactory for the density ratios used.

The assumptions and method of analysis are similar to that employed in section 3.2. Case II. That is, constant overall pressure drop, constant gas flow rate, homogeneous flow and unity slip ratio are assumed, and gas density with respect to liquid density and gas mass flow rate with respect to liquid mass flow rate and gravitational effects are neglected. A lumped parameter analog computer program will be used to study the flow.

3.3.1. Mass continuity

Using the approach employed in section 3.2, but normalizing with respect to the inlet conditions at onset

of instability instead of the exit conditions, the normalized mass continuity equation for the n^{th} lump becomes,

$$r_n u_n - r_{n+1} u_{n+1} = v_n \frac{d}{dT} (r_n + r_{n+1}) \quad \ldots\ldots (80)$$

where, $r = \frac{\text{Local Density}}{\text{Inlet Density}} = \frac{\rho n}{\rho_1}$

$$u = \frac{\text{Local Velocity}}{\text{Inlet Velocity}} = \frac{U_n}{U_{1s}}$$

$$v = \frac{\text{Lump Volume}}{\text{Mixer Volume}} = \frac{V_n}{V_m}$$

$$= \frac{Ln}{L_m} \text{ for uniform cross sectional area}$$

$$T = \frac{2\ U_{1s}\ A_1}{V_m} \cdot t$$

$$= \frac{2\ U_{1s}}{L_m} \cdot t \quad \text{for uniform cross-sectional area}$$

At steady-state, equation (80) results in,

$$r_{(n+1)s}\ u_{(n+1)s} = r_{ns}\ u_{ns} = r_1\ u_{1s} = 1 \quad \ldots\ldots (81)$$

since $r_1 = 1$ and $u_{1s} = 1$.

3.3.2. Volume continuity

Considering volume flow rates, the normalized volume continuity equation for a mixer lump becomes,

$$u_{n+1} - u_n = q \quad \ldots\ldots\ldots\ldots\ldots\ldots\ldots\ldots (82)$$

where $q = \frac{\text{Gas Volume Flow Rate into Lump}}{U_{1s} A_1} = \frac{Q}{U_{1s} A_1}$

For the inlet ducting and the exit ducting lumps, equation (82) reduces to,

$$u_{n+1} - u_n = 0 \quad \ldots\ldots(83)$$

since no gas is introduced into these lumps and gas compressibility is neglected.

At steady state the difference between the normalized exit and inlet flow velocities, from equations (82) and (83), becomes,

$$u_{4s} - u_{1s} = 2q$$

$$\text{or} \quad u_{4s} - 1 = 2q \quad \ldots\ldots(84)$$

since $u_{1s} = 1$.

From equation (81), the overall density ratio for steady state is given by,

$$r_{4s} = \frac{1}{U_{4s}} \quad \ldots\ldots(85)$$

Substituting equation (84) in (85),

$$r_{4s} = \frac{1}{1 + 2q} \quad \ldots\ldots(86)$$

It may be pointed out that the overall density ratios defined here and earlier in sections 3.1. and 3.2. are inverse of each other, i.e., $r_{4s} = 1/r_{is}$.

3.3.3. Pressure drop

The pressure drop relationship is considered in more detail than section 3.2. Consequently, the complete

derivation will be given.

In calculating the total pressure drop, the system was divided into three sections - the first consisting of the entrance ducting and inlet valve where there is no density change (lump 0), the second consisting of the mixer and the exit ducting where large density and velocity changes take place (lumps 1 through 3), and the third being the exit orifice.

For an incompressible liquid, the pressure drop $(P_o - P_1)$ across the lump 0 is the sum of the frictional pressure drop in the ducting, the pressure drop across the inlet valve and the inertial pressure drop, i.e.,

$$P_o - P_1 = K_o' \rho_1 U_1^2 + K_o'' \rho_1 U_1^2 + L_i \rho_1 \frac{dU_1}{dt} \quad \ldots\ldots (87)$$

where the coefficient K_o' is a function of the inlet ducting configuration and roughness, the coefficient K_o'' a function of the valve opening, and the length L_i the equivalent length for the inlet ducting. The equivalent length L_i is given by

$$L_i = A_1 \Sigma \frac{L}{A}$$

where $\Sigma(L/A)$ is summed for all the entrance ducting.

Similarly, for a constant cross-sectional-area mixer and exit ducting the pressure drop is,

$$P_1 - P_4 = \text{frictional pressure drop} + \text{momentum pressure drop} + \text{inertial pressure drop}$$

or

$$P_1 - P_4 = K_{me} \left(\frac{\rho_1 U_1^2 + \rho_4 U_4^2}{2}\right) + \left(\rho_4 U_4^2 - \rho_1 U_1^2\right)$$

$$+ L_{me} \frac{d}{dt} \left(\frac{\rho_1 U_1 + \rho_4 U_4}{2}\right) \quad \ldots\ldots\ldots\ldots\ldots\ldots (88)$$

where

$$K_{me} = \frac{4 f_{me} L_{me}}{D_{me}}$$

L_{me} = Mixer length plus exit ducting length,

f_{me} = Effective coefficient of friction for the mixer and exit ducting,

and D_{me} = Hydraulic diameter for the mixer and exit ducting.

The pressure drop across the exit orifice is expressed by the equation,

$$P_4 - P_5 = K_4 \rho_4 U_4^2 \quad \ldots\ldots\ldots\ldots\ldots\ldots\ldots (89)$$

assuming that a relationship of this type is still useful for two-phase flow.

Let us now normalize the pressure-drop equations with respect to the steady-state pressure at station 1, P_{1s}. Dividing equation (87) by P_{1s} and normalizing U_1, the normalized inlet pressure drop becomes,

$$p_o - p_1 = \frac{(K_o' + K_o'')\rho_1 U_{1s}^2 u_1^2}{P_{1s}} + \frac{L_i \rho_1 U_{1s}}{P_{1s}} \cdot \frac{du_1}{dt}$$

$\ldots\ldots\ldots\ldots\ldots (90)$

where

$$p = \frac{P}{P_{1s}}$$

and

$$u_1 = \frac{U_1 A_1}{U_{1s} A_1} = \frac{U_1}{U_{1s}}$$

Introducing the normalized time T and normalizing L_i with respect to the mixer length L_m reduce equation (90) to,

$$p_o - p_1 = (K_o' + K_o'') p'_d u_1^2 + 2\ell_i p'_d \frac{du_1}{dT} \quad \ldots\ldots (91)$$

where the normalized length of inlet ducting is given by

$$\ell_i = \frac{L_i}{L_m}$$

and the dynamic pressure normalized with respect to P_{1s}, is defined as

$$p'_d = \frac{\rho_1 U_{1s}^2}{P_{1s}}$$

At steady state, equation (91) yields

$$(K_o' + K_o'') p'_d = p_o - 1 \quad \ldots\ldots\ldots\ldots\ldots\ldots (92)$$

Substituting equation (92) in (91),

$$p_o - p_1 = (p_o - 1) u_1^2 + 2\ell_i p'_d \frac{du_1}{dT} \quad \ldots\ldots\ldots\ldots (93)$$

Dividing equation (88) by P_{1s}, and rearranging, one obtains,

$$p_1 - p_4 = \frac{(K_{me} - 2) p'_d}{2} u_1^2 + \frac{(K_{me} + 2) p'_d}{2} r_4 u_4^2$$

$$+ (1 + \ell_e) p'_d \frac{d}{dT} (u_1 + r_4 u_4) \quad \ldots\ldots\ldots\ldots\ldots\ldots (94)$$

where the normalized exit ducting length is defined as

$$\ell_e = \frac{\text{Exit ducting length}}{\text{Mixer length}} = \frac{L_e}{L_m}$$

At steady state, equation (94) yields

$$K_{me} = \frac{2(1 - p_{4s})\ r_{4s} + 2(r_{4s} - 1)\ p'_d}{(1 + r_{4s})\ p'_d} \quad \ldots\ldots\ldots\ldots (95)$$

Substituting equation (95) in (94), the normalized pressure drop across the mixer plus duct becomes

$$p_1 - p_4 = \frac{(1 - p_{4s})\ r_{4s} - 2\ p'_d}{1 + r_{4s}}\ u_1^2$$

$$+ \frac{(1 - p_{4s})\ r_{4s} + 2\ r_{4s}\ p'_d}{1 + r_{4s}}\ r_4\ u_4^2$$

$$+ (1 + \ell_e)\ p'_d\ \frac{d}{dT}\ (u_1 + r_4\ u_4) \quad \ldots\ldots\ldots\ldots (96)$$

Similarly the normalized form of equation (89) becomes

$$p_4 - p_5 = (p_{4s} - p_5)\ r_{4s}\ r_4\ u_4^2 \quad \ldots\ldots\ldots\ldots (97)$$

Summing up equations (93), (96), and (97) and thereby eliminating the variables p_1 and p_4, the total normalized pressure drop across the system becomes

$$p_o - p_5 = \left[\ p_o - \frac{1 + r_{4s}\ p_{4s} + 2\ p'_d}{1 + r_{4s}}\ \right] u_1^2$$

$$+ \left[\ \frac{(1 - p_{4s})\ r_{4s} + 2\ r_{4s}\ p'_d}{1 + r_{4s}} + (p_{4s} - p_5)\ r_{4s}\right] r_4\ u_4^2$$

$$+ p'_d\ \frac{d}{dT}\ [\ (1 + \ell_e + 2\ \ell_i)u_1 + (1 + \ell_e)r_4\ u_4] \ldots\ldots (98)$$

Noting that $p'_d \ll 1$, $r_{4s} < 1$ and assuming a relatively large pressure drop across the exit orifice compared to that of the mixer and exit ducting (i.e., $P_{4s} \approx 1$), we can reduce equation (98) to

$$p_o - p_5 = (p_o - 1)\, u_1^2 + (1 - p_5)\, r_{4s}\, r_4\, u_4^2$$

$$+ p'_d \frac{d}{dT} [(1 + \ell_e + 2\,\ell_i)\, u_1 + (1 + \ell_e) r_4\, u_4] \ldots\ldots (99)$$

Dividing both sides of equation (99) by the normalized constant pressure drop across the system, $p_o - p_5$, one obtains,

$$1 = y\, u_1^2 + (1 - y) r_{4s}\, r_4\, u_4^2$$

$$+ p_d \frac{d}{dT} [(1 + \ell_e + 2\ell_i) u_1 + (1 + \ell_e) r_4\, u_4] \ldots\ldots (100)$$

where

$$y = \frac{P_o - P_{1s}}{P_o - P_5}$$

the pressure drop fraction attributable to the upstream side, and

$$p_d = \frac{\rho_1\, U_{1s}^2}{P_o - P_5}$$

the dynamic pressure normalized with respect to the overall pressure drop.

3.3.4. Analog computation

In order to evaluate the conditions at onset of instability, equations (80), (82), (83), (86) and (100) were programmed on an EAI TR-48 analog computer. The equations were not linearized. As seen from the equations,

there are five variables governing stability; namely, the normalized inlet ducting length $\ell_i = L_i/L_m$, the normalized exit ducting length $\ell_e = L_e/L_m$, the steady state overall density ratio $r_{4s} = \rho_{4s}/\rho_1$, inlet pressure drop fraction $y = (P_o - P_{1s})/(P_o - P_5)$, and the normalized steady-state dynamic pressure, $p_d = (\rho_1 U_{1s}^2)/(P_o - P_5)$. It can be seen that it is convenient to fix the values of ℓ_i, ℓ_e, p_d, and y, and to vary the overall density ratio r_{4s} to obtain the onset of instability since r_{4s} can be controlled by means of one potentiometer only with no other adjustments needed. Consequently, during each series of computer runs the parameter r_{4s} was varied to obtain its value at the stability boundary while the remaining variables were kept constant. The onset of instability was determined by observing an oscilloscope image of density (or velocity) voltage at one of the stations, usually the station at the end of the mixer, and adjusting the density ratio r_{4s} until small oscillations were barely visible. No hysteresis effect was noted, that is the stability boundary was the same when approached from the stable or unstable sides. Altogether 57 series of computer runs were carried out. The values of ℓ_i used were between 0.5 and 8, ℓ_e between 0.2 and 5, $1/r_{4s}$ between 3 and 13, y between 0 and 0.26, and p_d between 0 and 0.03. These values were selected to cover the range of parameters encountered in the air-water experiments.

3.3.5. Computer results

The analog computer results are plotted in Figs. 10 through 18. The region above each curve is unstable, and below each curve is stable.

Fig. 10 shows the relationship between the overall density ratio $\rho_1/\rho_{4s}(=1/r_{4s})$ and the normalized inlet ducting length ℓ_i at the stability boundary for different values of the inlet pressure drop fraction y with p_d constant and equal to 0.015, and ℓ_e constant and equal to 1.5. With the exception of a small counter trend for low values of ℓ_i at y = 0.13, increasing the length of the inlet ducting increases the range of density ratios for which the system is stable. Since the fluid inertia (and hence the resistance to flow changes) of the system increases with ℓ_i, this trend is not surprising.

In Fig. 11, the effect of exit ducting length ℓ_e on stability is shown for p_d = 0.015, ℓ_i = 4.5. In general, the range of stable density ratios decreases at a decreasing rate as the exit ducting length is increased. For higher values of inlet pressure drop (or higher values of overall density range), the range of stable density ratios starts increasing - after hitting a minimum - with further increase in the exit ducting length.

Figs. 12 through 18 show the stability maps - the relationship between ρ_1/ρ_{4s} and p_d at the stability boundary - for various comibinations of ℓ_i, ℓ_e and y. The parameter p_d

enters the equations as a factor in the effective fluid inertia, and hence an increase in p_d helps to stabilize the system. The small destabilizing trend sometimes found at low values of p_d is unexpected and may be a consequence of small cumulative errors in the computer. Increasing the inlet side pressure drop always helps to stabilize the system, due to the damping effect on flow changes.

3.3.6. Conclusions

From the above analysis of a two-component two-phase flow system consisting of some inlet ducting, an inlet flow restriction, a mixer, some exit ducting and an exit flow restriction, the following conclusions are arrived at:

a. In general, increase in normalized inlet ducting length increases stability. For combinations of high inlet pressure drop and small inlet ducting length there is a slight counter effect.

b. In general, increase in normalized exit ducting length decreases stability. For combinations of high inlet pressure drop and large inlet ducting length, there is a slight counter effect.

c. In general, increase in inertia increases stability. For combinations of low inertia and small exit ducting length, there is a slight counter effect.

d. Increase in inlet pressure drop increases stability.

e. Increase in overall density ratio decreases stability.

The above conclusions are in agreement with the comparable conclusions of section 3.2., but are of more general nature.

4. EXPERIMENTAL STUDIES

In experiments, a test section similar to the model used for the theoretical studies (Case III) was used. Air and water were selected as the two-phase flow components since they were readily available in the laboratory. The experiments carried out could conveniently be divided into three parts: the experiments for determining orifice characteristics, the experiments for determining slip ratios, and the experiments to investigate conditions at onset of instability.

4.1. Experimental Apparatus

In order to obtain a well-mixed (homogeneous) two-component two-phase flow as was assumed in the analysis, it was decided to have a vertical flow. And, because of convenience, the direction of the flow was selected as downward. Consequently the test sections were designed for a downward two-component two-phase flow.

The air-water two-phase flow test section used in the orifice characteristics and instability experiments is shown in Fig. 19. It consisted of a surge tank, some inlet ducting, an inlet valve, a mixer, some exit ducting and an exit orifice. Water entered the test section from the surge tank at pressures up to 40 psig and flowed through the inlet ducting and inlet valve into the inner tube of the mixer. The pressurized air supplied to the jacket of the mixer seeped through the porous bronze inner tube and bubbled into the water. The two-phase

mixture then flowed through the exit ducting and out of the rounded exit orifice. The pressure drop across the walls of the porous bronze tube was so large (about 40 psi) that the air flow rate was insensitive to oscillations in test section pressure.

The surge tank damped out any fluctuations in the water supply and provided a constant pressure drop across the test section, while the inlet valve was used to control the inlet pressure drop. The exit duct was made of clear lucite tube for observation of the two-phase flow and the oscillations. It was prepared in several lengths up to 22 in. with an inner diameter of 5/8 in., the same as that of the porous bronze tube in the mixer. To study the effect of orifice size, three exit orifice pieces were constructed with 1/8, 3/16 and 1/4 in. diameter nozzles.

Fig. 20 shows the complete experimental set-up and the instrumentation for the orifice characteristics and instability experiments. Air was supplied through the high-pressure, compressed-air system in the laboratory, which provided air at constant pressure, and water was circulated by a motor-driven centrifugal pump. Air and water flow rates were controlled by a needle valve and a wedge-gate valve, respectively. The water flow rate was measured by a Potter turbine-type flowmeter and the air flow rate by a Vol-O-Flow flowmeter. Bourdon-type Heise pressure gages were used to measure the pressures

along the inlet ducting, in the air jacket and at other stations as indicated in the sketch. To observe and record the two-phase flow oscillations, two Giannini pressure transducers were placed at the upstream and downstream sides of the lucite outlet tubing. These pressures were recorded on two Esterline-Angus chart recorders, and fluctuations in water flow rate were also recorded on a chart recorder.

For the slip ratio experiments, a special test section in place of the exit tubing was used. Fig. 21 shows this special test section together with the rest of the experimental set-up. The test section was made of a vertical clear lucite tube of 5/8 inch inside diameter and 26 inches long. It was fitted with two ball valves of 3/4 inch opening diameter, one at each end. The two ball valves were connected with a parallelogram mechanism with one handle so that both the valves could be operated simultaneously. A 90^{o} turn was enough to change the position of the valves from "open" to "closed" or vice-versa. The upstream side of the test section was connected to the mixer and the downstream side was connected to a plastic tube having an inner diameter of 5/8 inch, which had a 3/16 inch diameter round edged exit orifice clamped to it. The position of the exit orifice could be changed up to 2 feet from the test section in order to investigate the orifice entrance effect on slip-ratio.

4.2. Orifice Characteristics Experiments

In equations (16), (63) and (89) of the analysis it was assumed that the usual orifice equation applicable to one component fluid flow is also good for two-component two-phase fluid flow. In order to verify this assumption a series of experiments were carried out.

4.2.1. Experimental procedure

At the beginning of each experiment air was first run through the system at a low flow rate, and then the water pump was started. This prevented water from entering the air jacket. After this precaution, air and water at various proportions (in order to obtain various mixture densities) were run through the orifice at steady state up to the onset of the instability. The orifice pressure drop and the air and water flow rates and temperatures were recorded. This procedure was repeated for each of the three orifice pieces.

4.2.2. Experimental results

The results of the experiments are plotted in Figs. 22 through 24 for each orifice size as the mean two-phase velocity at exit, U_{4s}, versus orifice pressure drop divided by mixture density at exit, $\frac{\Delta p_{or}}{\rho_{4s}}$. The orifice equations obtained from the best line through the experimental points are given in the Figures. In the conventional orifice equation, U_{4s} is proportional to $(\frac{\Delta p_{or}}{\rho_{4s}})^{0.5}$.

As seen from the Figures, the 1/8" diameter orifice had a flow characteristic close to the assumed relation, with an exponent of 0.485 instead of 0.5. The 3/16" diameter

orifice also gave fair agreement with the assumed relation, with an exponent of 0.474. The departure from the assumed relation was largest in the case of the 1/4" diameter orifice. Consequently, it would be expected that the best agreement between theory and experiments would be obtained with the two smaller orifices.

4.3 Slip Ratio Experiments

A series of experiments were carried out to see to what extent the assumption of unity slip ratio employed in the analysis would hold.

4.3.1. Experimental procedure

In these experiments, as in the orifice characteristics experiments, air was first run through the system at a low flow rate, and then the water pump was started with test section valves in the open position. This prevented water from entering the air jacket. After this, the water flow rate was brought up to a predetermined value by adjusting the water control valve. The pressurized air supplied to the jacket of the mixer seeped through the porous bronze tube and bubbled into the water passing through the tube. The two-phase mixture formed in the mixer then flowed through the test section and out of the exit orifice. The flow observed in the test section was well mixed and bubbly.

After making sure that the air and water flow rates were steady, room temperature, barometric pressure, air and water flow rates and the pressures at various stations

were recorded. Soon after taking the readings, the two test section valves were closed simultaneously by means of the parallelogram mechanism. (The surge tank eliminated the water hammer action which otherwise would have resulted from abrupt closing of the ducting.) After the separation of air and water in the test section, the water level was noted. This procedure was repeated for increasing air flow rates up to the onset of the two-component two-phase flow oscillations, by re-adjusting the water control valve at each step so that the water flow rate was kept constant. The experiments were not carried into the unstable region, since it was then not possible to obtain a uniform mixture in the test section.

The above described procedure was repeated for various water flow rates. In all the experiments the inlet valve was kept fully open.

Some preliminary tests were run with the exit orifice placed at distances varying from 2 inches to 2 feet from the downstream valve of the test section. No noticeable effect on slip was observed.

4.3.2. Experimental results

Using the readings taken during each experiment, the void fraction, the density ratio of the water density to that of the mixture and the slip ratio (i.e., the ratio of gas velocity to liquid velocity) were calculated. The results are plotted in Figs. 25 and 26 as slip versus density

ratio and slip versus void fraction respectively. From Fig. 25 it can be seen that for a downward air-water two-phase flow (a) the slip ratio decreases and tends asymptotically towards one as density ratio increases, and (b) the slip ratio decreases as liquid (in this case water) flow rate increases. Because of a directly varying relationship between the void fraction and the density ratio, the above observations also apply to the slip ratio versus void fraction relationship (see Fig. 26).

In the instability experiments with the air-water two-phase flows, the density ratios at the onset of instabilities ranged from 3 to 11. From Fig. 25, it can be seen that for this density ratio range, the slip ratio would be of the order of one (between 1 and 1.5). In other words, for air-water two-phase downward flow experiments the assumption of unity slip ratio is justifiable.

4.4. Instability Experiments

In order to investigate the relationship between the flow parameters at onset of instability, a series of experiments have been carried out.

4.4.1. Experimental procedure

At the beginning of each experiment air was run through the system at a low flow rate, and then water was allowed to flow and its flow rate was brought up to a predetermined value. After this, the air flow was increased in small steps till the onset of two-phase flow oscillations was observed. These oscillations could be

observed visually through the lucite exit tubing and also on the pressure recorders. At the stability boundary, reached from the stable region as just described, room temperature, barometric pressure, air and water flow rates and the pressures at various stations were recorded. Then the air flow rate was further increased to operate in the unstable region and to obtain chart recordings of the pressures for frequency calculations. In addition, the temperature, mean-flow and mean-pressure readings were taken. After this, by reducing the air flow the stability boundary was reached from the unstable region. A new set of readings also was taken at this stage. Experiments were repeated by varying the inlet pressure drops for each length of exit ducting and each orifice size.

A well-mixed bubbly flow was observed in the test section at steady-state operation. When the stability boundary was crossed, the water flow rate immediately began to oscillate with an amplitude roughly 40 percent of the mean flow rate (Fig. 27) and alternating bubbly slugs containing mostly air or mostly water were observed in the lucite duct. Reducing the mean water flow rate or increasing the air flow rate to move farther into the unstable regime produced some increase in the amplitude of the water flow oscillations, but little change in frequency. The air flow rate was unaffected by the oscillations, and the pressure in the test section oscillated with a maximum amplitude of approximately 1 psi. The frequency was of the order of

1 cps. Except for the 1/4 in. orifice, the pressure drop in the mixer and duct was less than 5 percent of the overall pressure drop.

4.4.2. Experimental results

Using the experimental readings, the overall density ratio $1/r_{4s}$ (water density divided by the mixture density at exit), normalized inlet pressure drop y (inlet pressure drop divided by the total pressure drop), time period of oscillations near stability boundary τ_o, mean exit mixture velocity U_{4s}, normalized inlet ducting length l_i, and normalized exit ducting length l_e were calculated. Figs. 28 through 38 show the plots of the overall density ratio versus the normalized inlet pressure drop at both the onset of the oscillations and during the oscillations for various exit ducting lengths and orifice sizes. There is no distinguishable hysteresis effect. Although there is some scattering of points at the boundary, it seems that the same mean boundary is obtained whether approached from the stable or unstable regions. All the points corresponding to unstable operation have a higher overall density ratio for a given y than the points at the stability boundary.

Fig. 39 shows the plots of the normalized time period of oscillations at the stability boundary as $\tau_o U_{4s}/L_{me}$ versus l_e for different values of y, where L_{me} is the total length of mixer plus exit ducting. The plots show that the normalized time period of oscillations increases with increasing y,

and decreases with increasing l_e and seems to reach a constant value asymptotically as l_e is increased.

5. COMPARISON OF EXPERIMENTS WITH THEORY

On Figures 28 through 38, the stability boundary curves obtained from the analysis are superimposed. The coordinates ($1/r_{4s}$, y) of the points of the theoretical curve were obtained from the theoretical stability maps (Figs. 12 through 18) corresponding to the parameters (l_i, l_e, p_d) of the experimental points. The points so determined were then plotted on the corresponding figures of the experimental results to obtain the theoretical curves. The value of l_i for the apparatus was 3.46.

The best experimental curve for the stability boundary is also drawn in each Figure. These curves were obtained by joining the experimental points nearer to the stable region (i.e., the points corresponding to lower overall density ratios for a given inlet pressure drop fraction) instead of drawing them through the mean of all the boundary points. This was done because, as explained above, the stability boundary depends on the detection of small oscillations by the observer. It is therefore expected that due to human error some of these "boundary" points may really be in the unstable region and the true stability boundary is probably the lower envelope of all the onset measurements. It should be noted that since no computer data was available for $l_e = 0$, the corresponding ($1/r_{4s}$ versus y) analytical curve could not be plotted in Figure 38.

In comparing the stability theory and the experimental results, the following observations can be made:

a. For small values of inlet pressure drop fraction y ($y < 0.08$) the agreement between the theory and the experiments is good. The divergence is less than $\pm$ 10%.

b. For values of inlet pressure drop fraction y between 0.08 and 0.16 the divergence is greater - up to 30%, the theoretical prediction of stability boundary being conservative; i.e., the actual systems are more stable than indicated by the theory. This could be caused by slip between the gas and liquid, which is neglected in the analysis, but there is no reason to expect slip effects to be more important in this region than at small values of y. The departure of the actual orifice characteristics from the theoretical equation tends to stabilize the system.

c. The theoretical and experimental stability curves meet at a value of inlet pressure drop fraction y around 0.16, and further closure of the inlet valve does not change the density ratio at which instability occurs. This behavior is at variance with the theoretical curves, which continue to show some increase in stability with increasing y. It is possible that cavitation occurred in the inlet valve for the higher values of inlet pressure drop, producing a vapor cavity which decoupled the valve flow from the flow oscillations in the test section.

A similar phenomenon was observed in the Freon boiling rig when cavitation occurred between the inlet valve and the boiler. With the 1/4" orifice, the minimum value of y attainable was 0.10, due to the relatively large effect of inlet piping losses with this configuration. In consequence, it was not possible to compare theory and experiment in the region of y where agreement was good for the 1/8" and 1/4" orifices. The stability boundary was completely insensitive to y for the 1/4" orifice, and since the water flow rate was greatest and the water pressure lowest (about 10 psig) for this configuration, inlet valve cavitation was most likely to occur with the 1/4" orifice.

Analog computer measurements of predicted oscillation frequency were made only for the case of zero inlet pressure drop, and these predictions are shown on Figure 39. Agreement with the experimental data is excellent, with a maximum error of 7% in the predicted frequency. Increasing the inlet pressure drop has the effect of increasing the dimensionless time period of the oscillations, due to the longer particle residence time which accompanies the increased density ratio at the stability boundary.

6. CONCLUSIONS

The assumed model of two-component two-phase transient flow behavior reproduces the major features of two-phase flow instability in a simple air-water system. The oscillations are caused by the dynamic interaction between flow, density distribution and pressure drop distribution within the mixer, and the sensitivity of flow to exit pressure and exit density. Over a wide range of the variables the density ratio for instability onset is predicted within 30 percent. The frequency of the oscillations at the start of instability is predicted within 7 percent for the case where theoretical values are avilable. Using the stability maps presented, the mode of operation (whether stable or unstable) could be predicted for a given single channel two-component two-phase flow system provided that the system geometry and flow parameters are within those ranges covered in the maps. Otherwise, the analytical method outlined could be used for predicting the mode of operation.

Further work on the detailed flow pattern in the test section is necessary to improve the accuracy in predicting the theoretical stability boundary. The theory could be refined, and hence the agreement with the experiments improved, (a) by using actual two-phase flow orifice characteristics, (b) by taking into account slip between gas and liquid flows, (c) by considering pressure distribution in more detail (instead of relating it only to inlet and exit flow conditions), and (d) by dividing the system into more lumps.

ACKNOWLEDGEMENTS

The work described in this report was sponsored by the National Aeronautics and Space Administration and directed by the authors. However, many other individuals made substantial contributions to the project. The principal participants were Mr. L. Arrondo, Mr. T. C. Wang and Mr. G. Callahan.

REFERENCES

1. A.H. Stenning and T.N. Veziroglu, "A Parametric Study of Boiling Instability", NASA Grant NsG-424 Report No. 1, September 1963.

2. A.H. Stenning and T.N. Veziroglu, "Semi-Annual Status Report on Boiling Flow Instability", NASA Grant NsG-424 Report No. 2, November 1963.

3. A.H. Stenning and T.N. Veziroglu, "Oscillations in Two-Phase Two-Component Flow", NASA Grant NsG-424 Report No. 4, October 1964.

4. A.H. Stenning and T.N. Veziroglu, "A Parametric Study of Boiling Instability", ASME paper 64-WA/FE-28, presented at the Winter Annual Meeting, December 1964.

5. A.H. Stenning and T.N. Veziroglu, "Oscillations in Two-Component Two-Phase Flow", ASME paper 65-FE-24, presented at the Applied Mechanics and Fluids Engineering Conference, June 1965.

6. A.H. Stenning and T.N. Veziroglu, "Semi-Annual Status Report on Boiling Flow Instability", NASA Grant NsG-424 Report No. 8, November 1965.

7. S.W. Gouse, "Two-Phase Gas-Liquid Flow Oscillations: Preliminary Survey", Engineering Projects Laboratory, Department of Mechanical Engineering, M.I.T. Report DSR 8734-5, July 1964.

REFERENCES (Continued)

8. J.E. Meyer and R.P. Rose, "Application of a Momentum Integral Model to the Study of Parallel Channel Boiling Flow Oscillations", Journal of Heat Transfer, Trans. ASME, Series C, Vol. 85, February 1963, pp. 1-9.

9. G.B. Wallis and J.H. Heasley, "Oscillations in Two-Phase Flow Systems", Journal of Heat Transfer, Trans. ASME, Series C, Vol. 83, August 1961, pp. 363-369.

10. A.H. Stenning, "Instabilities in the Flow of a Boiling Liquid", Journal of Basic Engineering, Trans. ASME, Series D, Vol. 86, June 1964, pp. 213-217.

NOMENCLATURE

Symbols:

A	flow area
C	constant
D	hydraulic diameter or diameter
f	coefficient of friction
K	constant, pressure drop constant
ℓ	normalized length
L	length
p	normalized pressure
P	pressure
q	normalized volume rate of gas injection
Q	volume rate of gas injection
r	normalized density
t	time
T	normalized time
T_r	mean residence time
u	normalized volume flow rate, normalized velocity
U	velocity
v	normalized volume
V	volume
x	distance
y	normalized upstream pressure drop
ϵ	amplitude
ρ	density
τ	normalized inertia parameter
τ_o	time period of oscillations
Φ	volume rate of gas injection per unit mixer volume
ω	angular velocity, circular frequency

Subscripts:

d	dynamic
e	exit, exit ducting
f	frictional
g	gas
i	inlet, inlet ducting
m	mixer, lumps in mixer, momentum
me	mixer plus exit ducting
n	lump number, station number
o	mean
or	orifice
r	residence
s	steady state
t	total

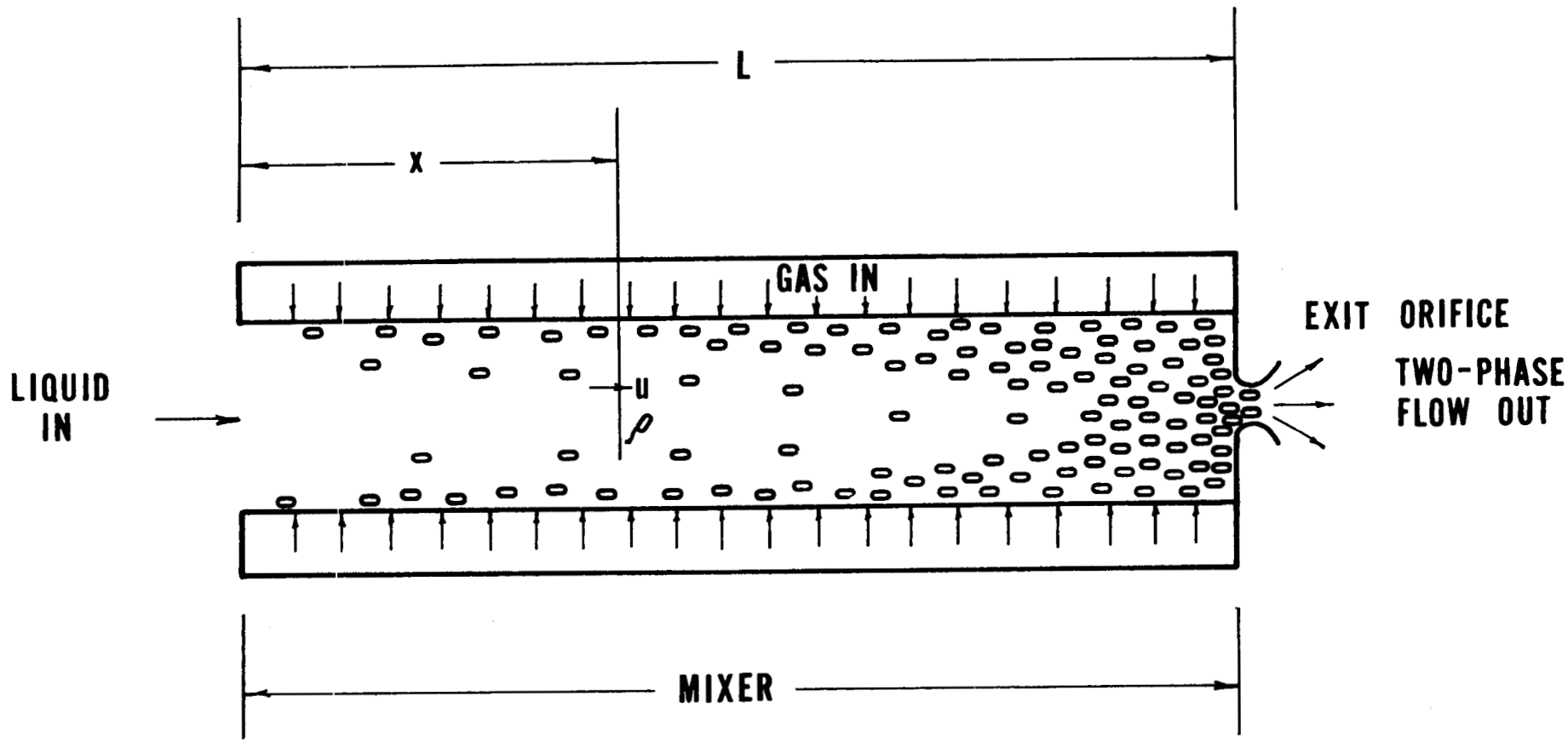

FIG. 1.- TWO-COMPONENT TWO-PHASE FLOW SYSTEM CONSIDERED UNDER CASE I

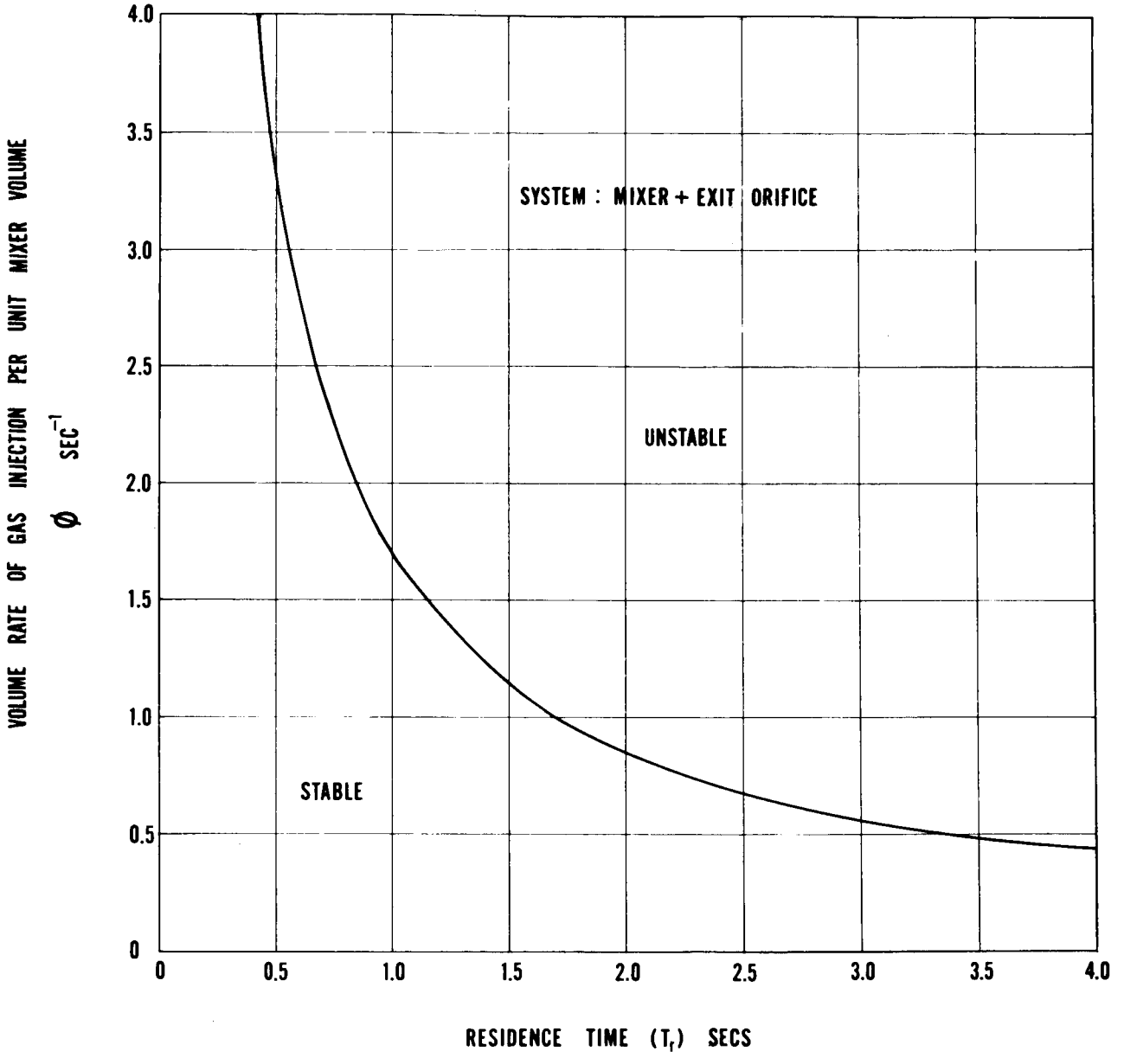

FIG. 2. – RESIDENCE TIME VS TIME RATE OF GAS INJECTION PER UNIT MIXER VOLUME AT ONSET OF OSCILLATIONS FOR CASE I

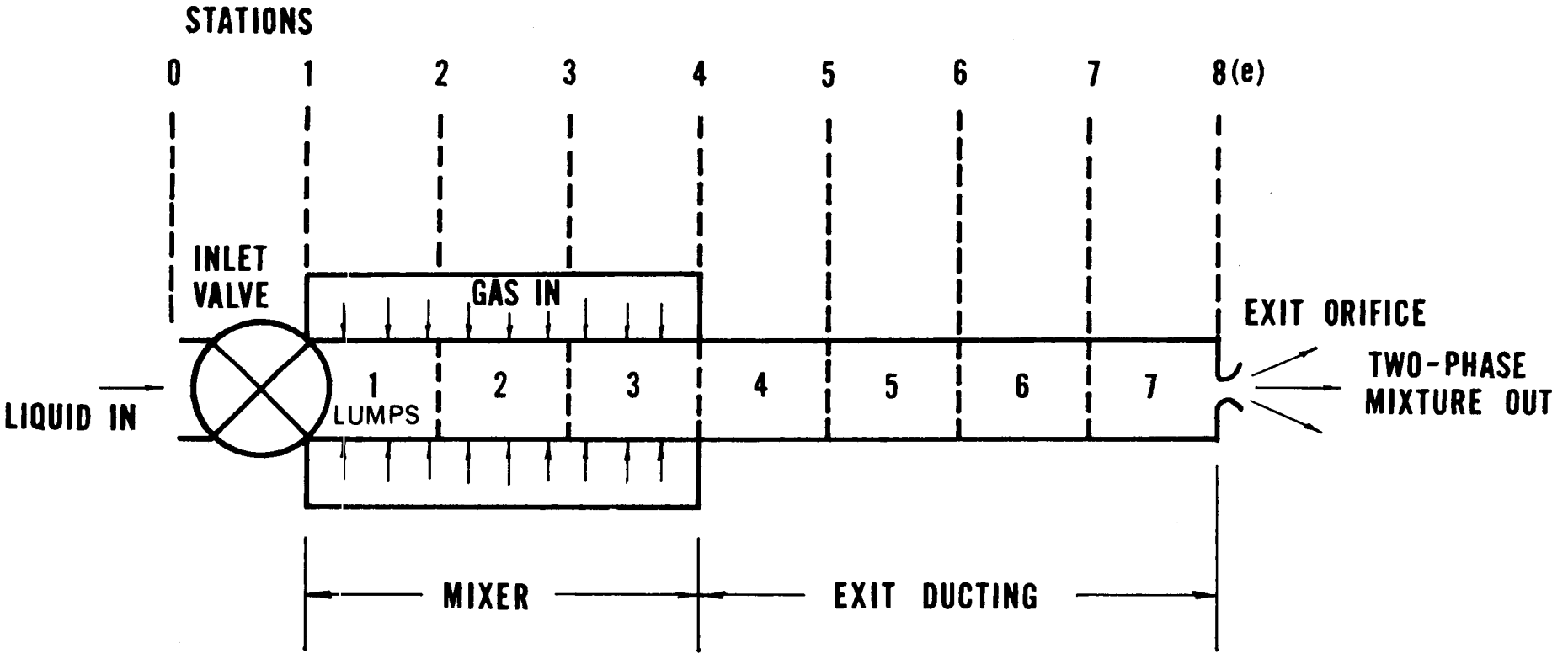

FIG. 3.– TWO-COMPONENT TWO-PHASE FLOW SYSTEM CONSIDERED UNDER CASE II

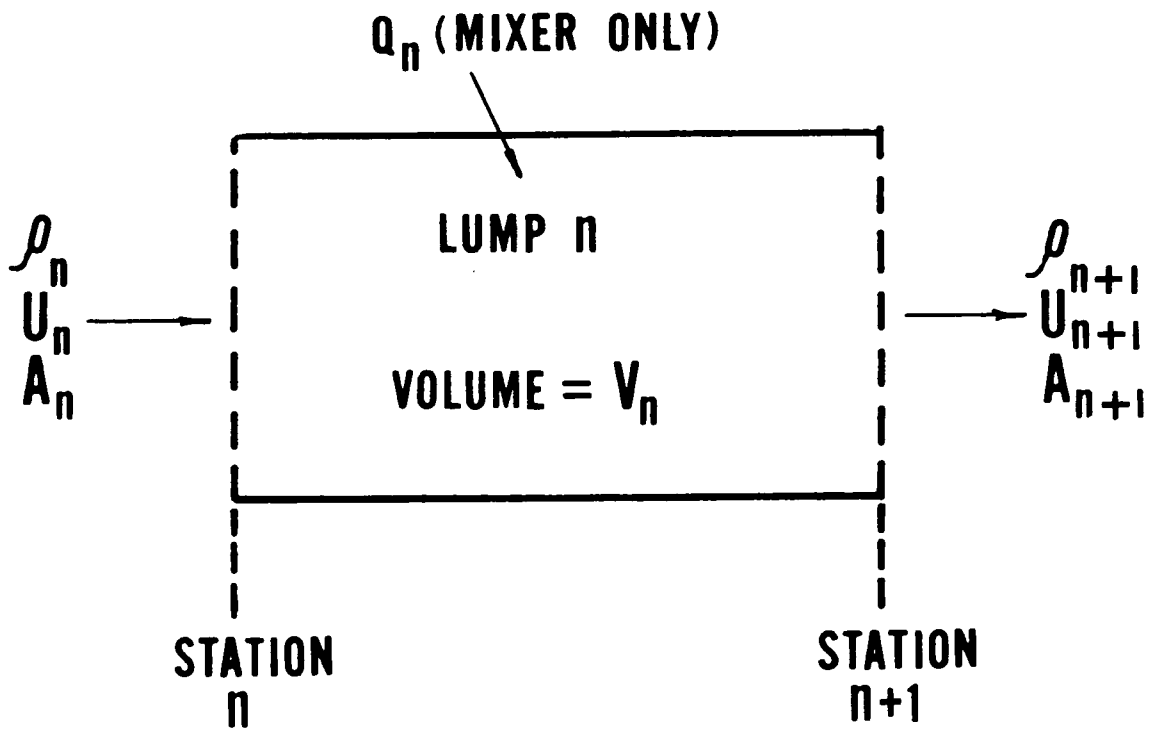

FIG. 4.– PORTION OF SYSTEM CONSIDERED UNDER CASE II

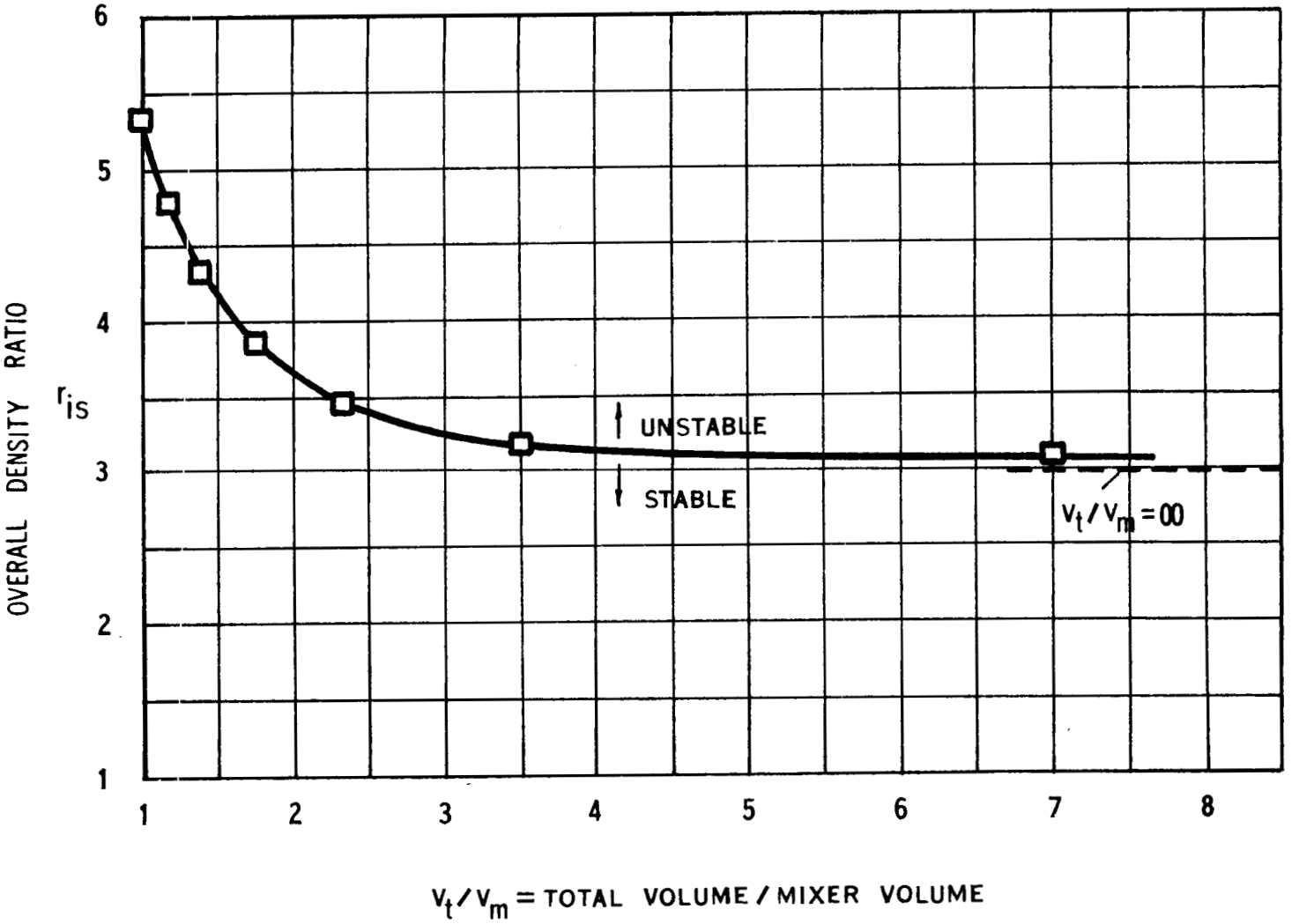

FIG. 5. – OVERALL DENSITY RATIO VS SYSTEM VOLUME TO MIXER VOLUME RATIO FOR CASE II WHEN Y=0 AND τ=0

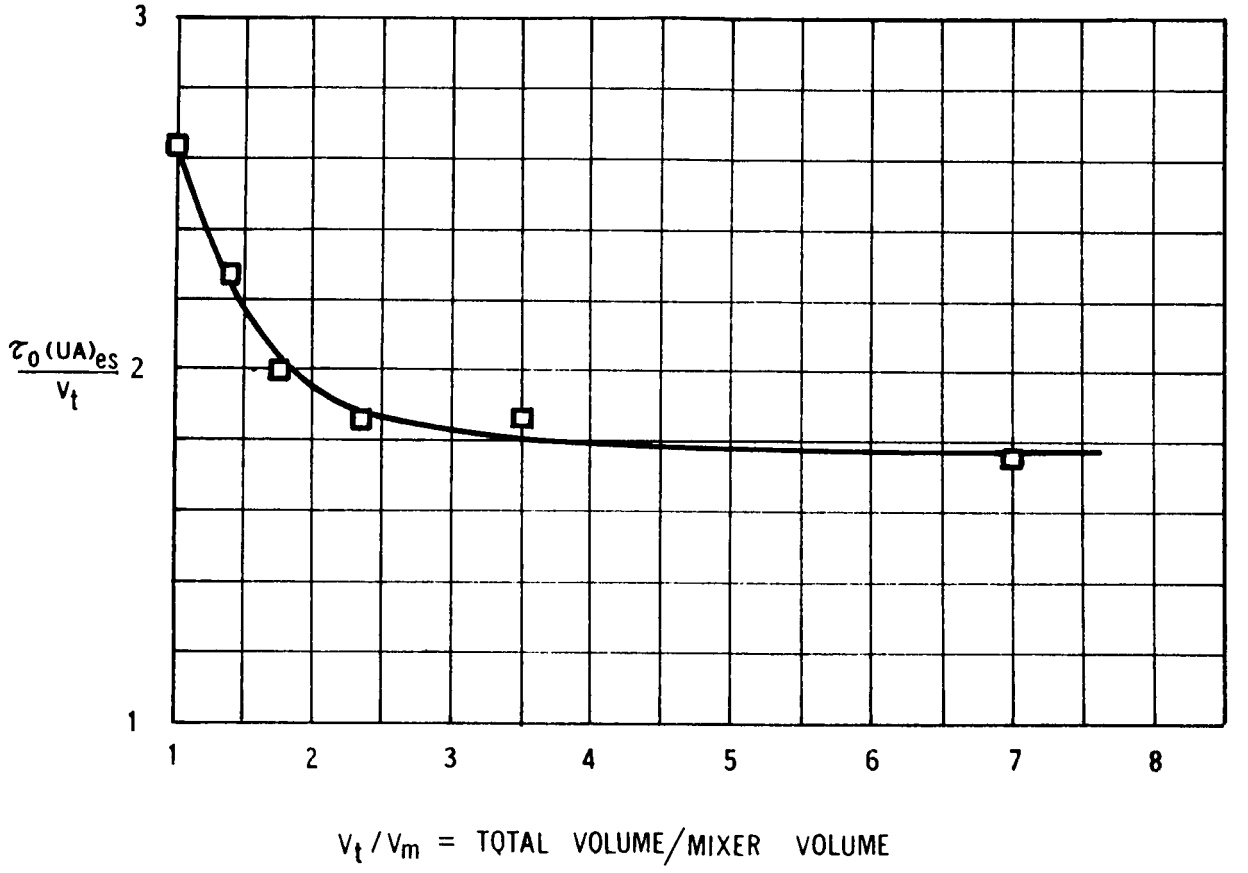

FIG. 6. – EFFECT OF SYSTEM VOLUME TQ MIXER VOLUME RATIO ON TIME PERIOD OF OSCILLATIONS AT STABILITY ONSET FOR CASE II WHEN $Y=0$ AND $\tau=0$

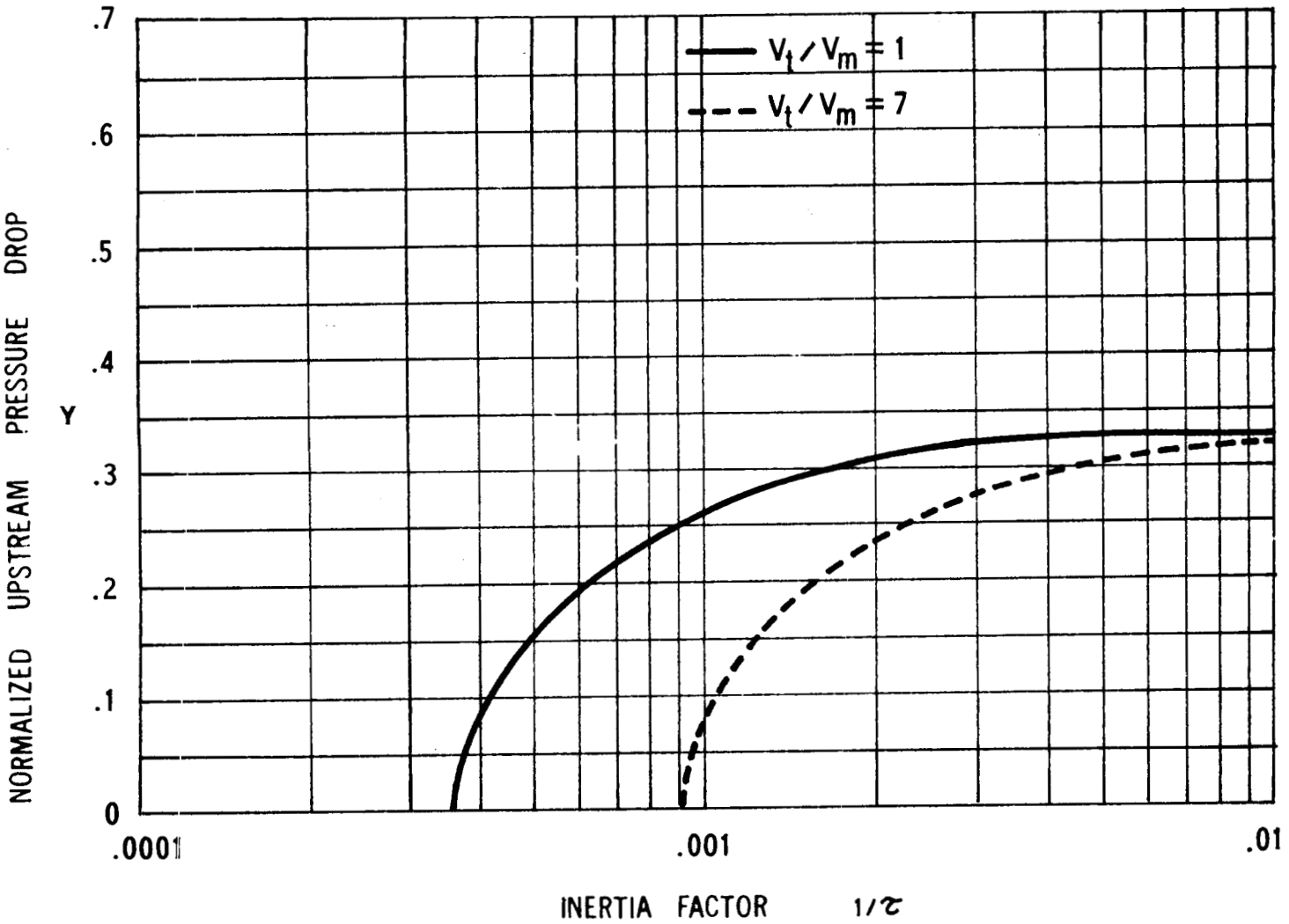

FIG. 7. – EFFECT OF SYSTEM VOLUME TO MIXER VOLUME RATIO ON STABILITY BOUNDARY FOR CASE II WHEN $r_{is} = 150$

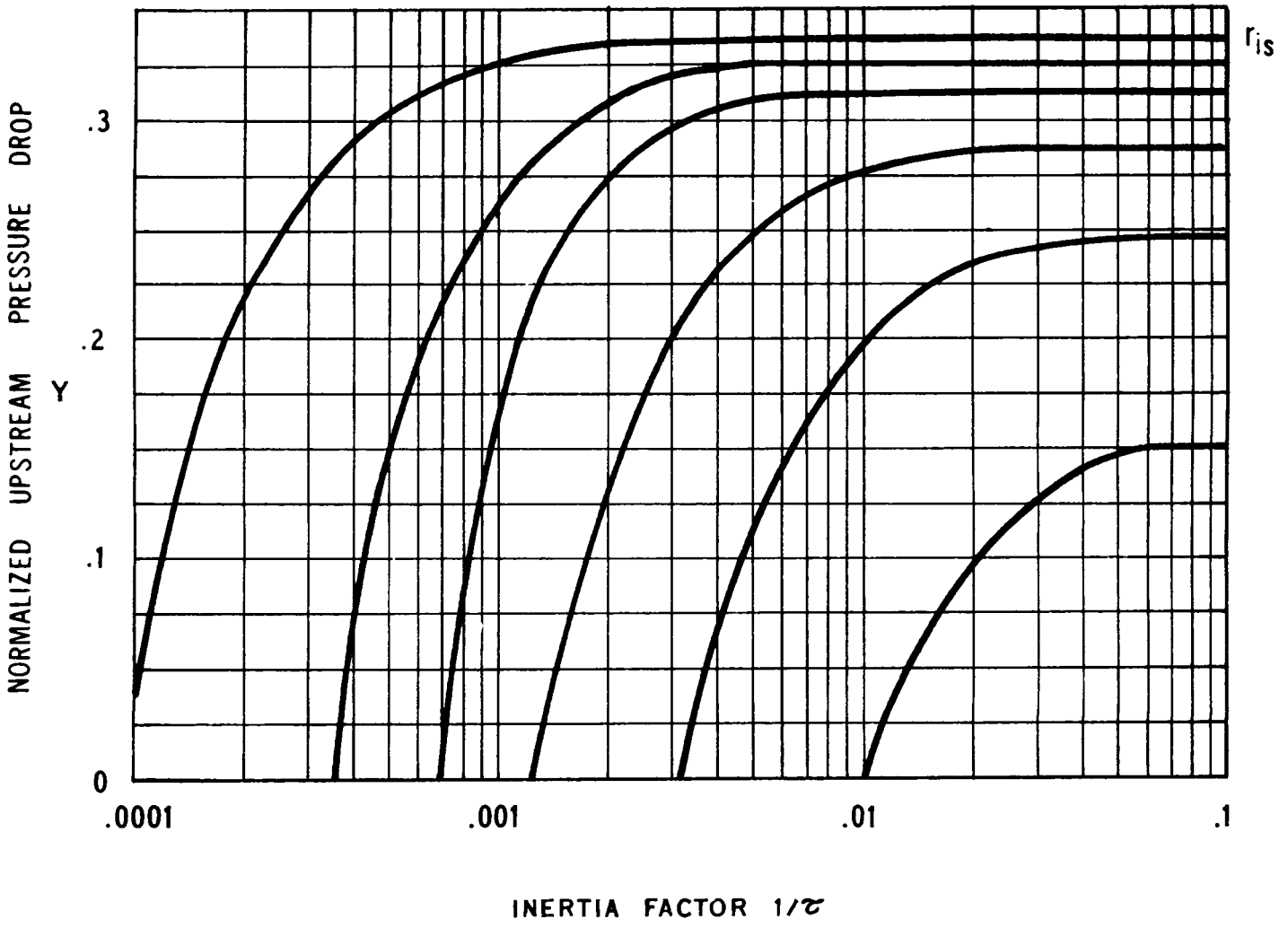

FIG. 8. – EFFECT OF OVERALL DENSITY RATIOS ON STABILITY BOUNDARY FOR CASE II WHEN $V_t / V_m = 1$

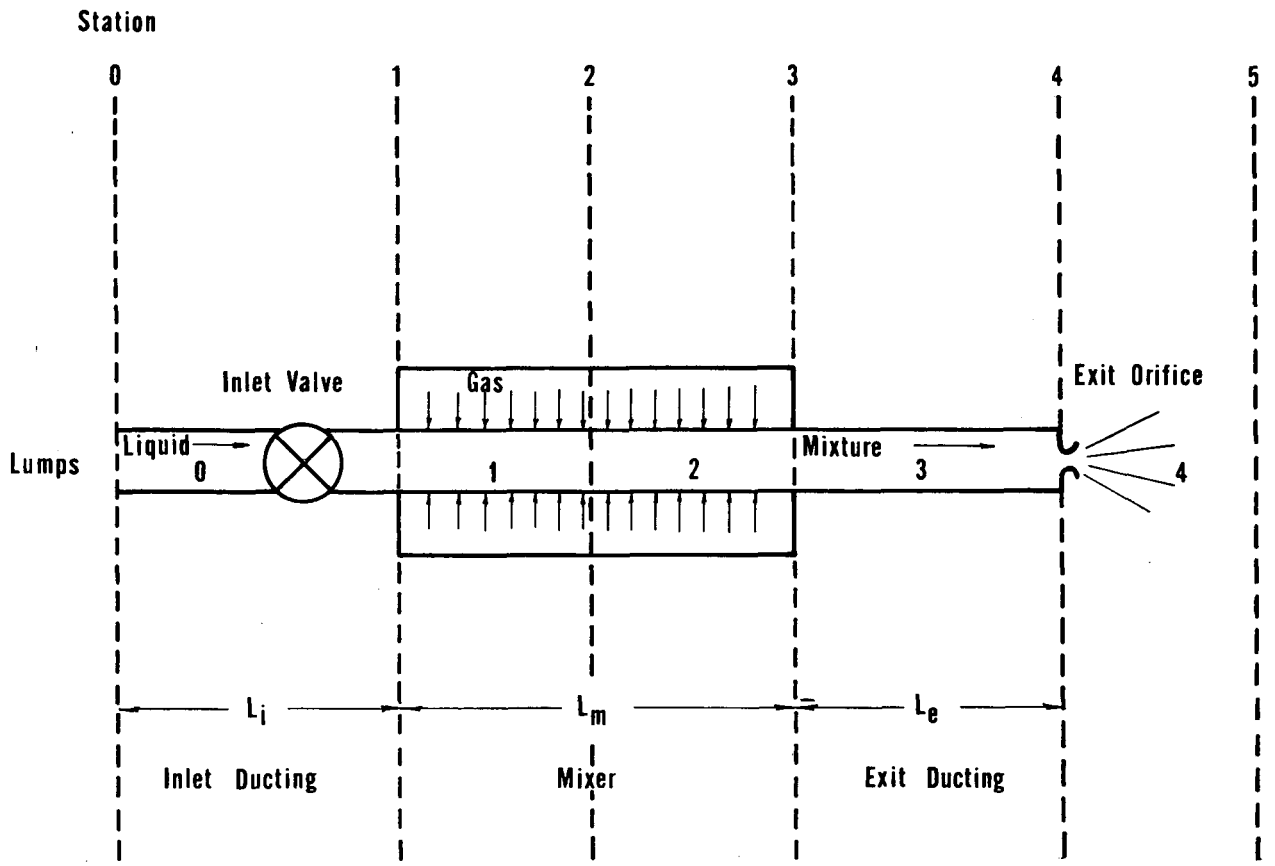

FIG. 9. - TWO-COMPONENT TWO-PHASE FLOW SYSTEM CONSIDERED UNDER CASE III

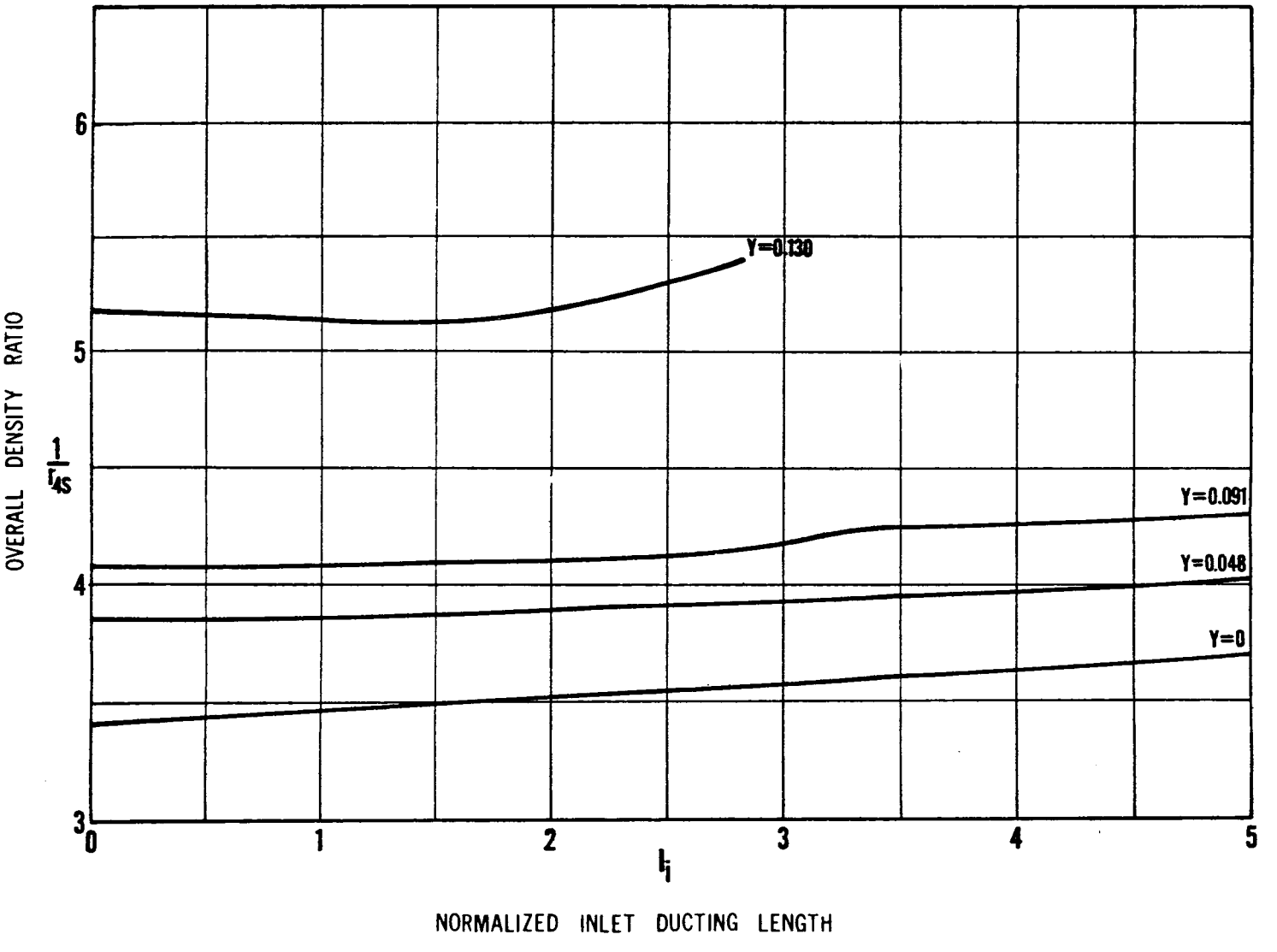

FIG.10.– OVERALL DENSITY RATIO VS NORMALIZED INLET DUCTING LENGTH AT STABILITY BOUNDARY (l_e=1.5, P_d=0.015)

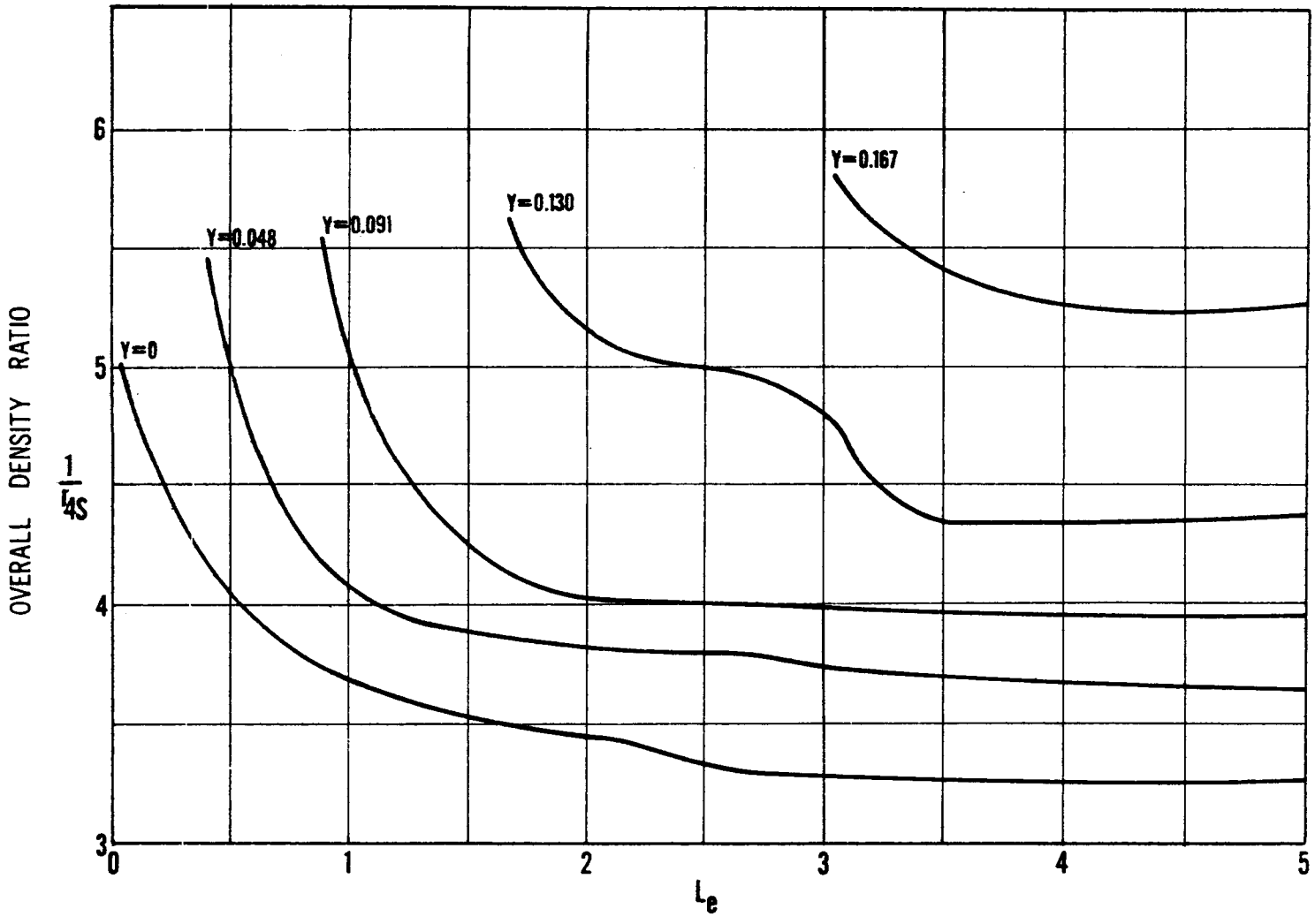

FIG.11.–OVERALL DENSITY RATIO VS NORMALIZED EXIT DUCTING LENGTH AT STABILITY BOUNDARY
(I_i=4.5, P_d=0.015)

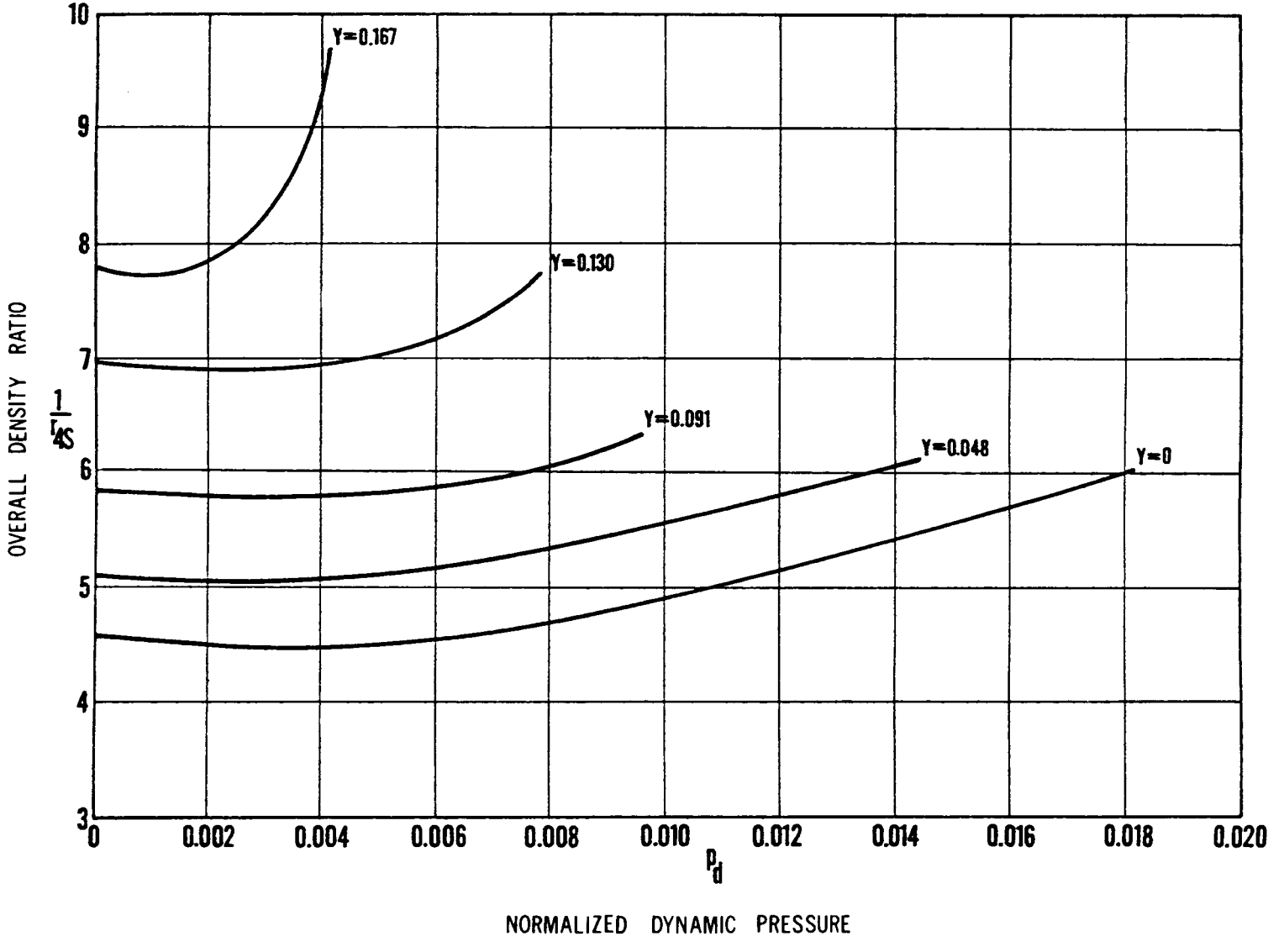

FIG.12–OVERALL DENSITY RATIO VS NORMALIZED DYNAMIC PRESSURE AT STABILITY BOUNDARY
($l_i = 2.5$, $l_e = 0.2$)

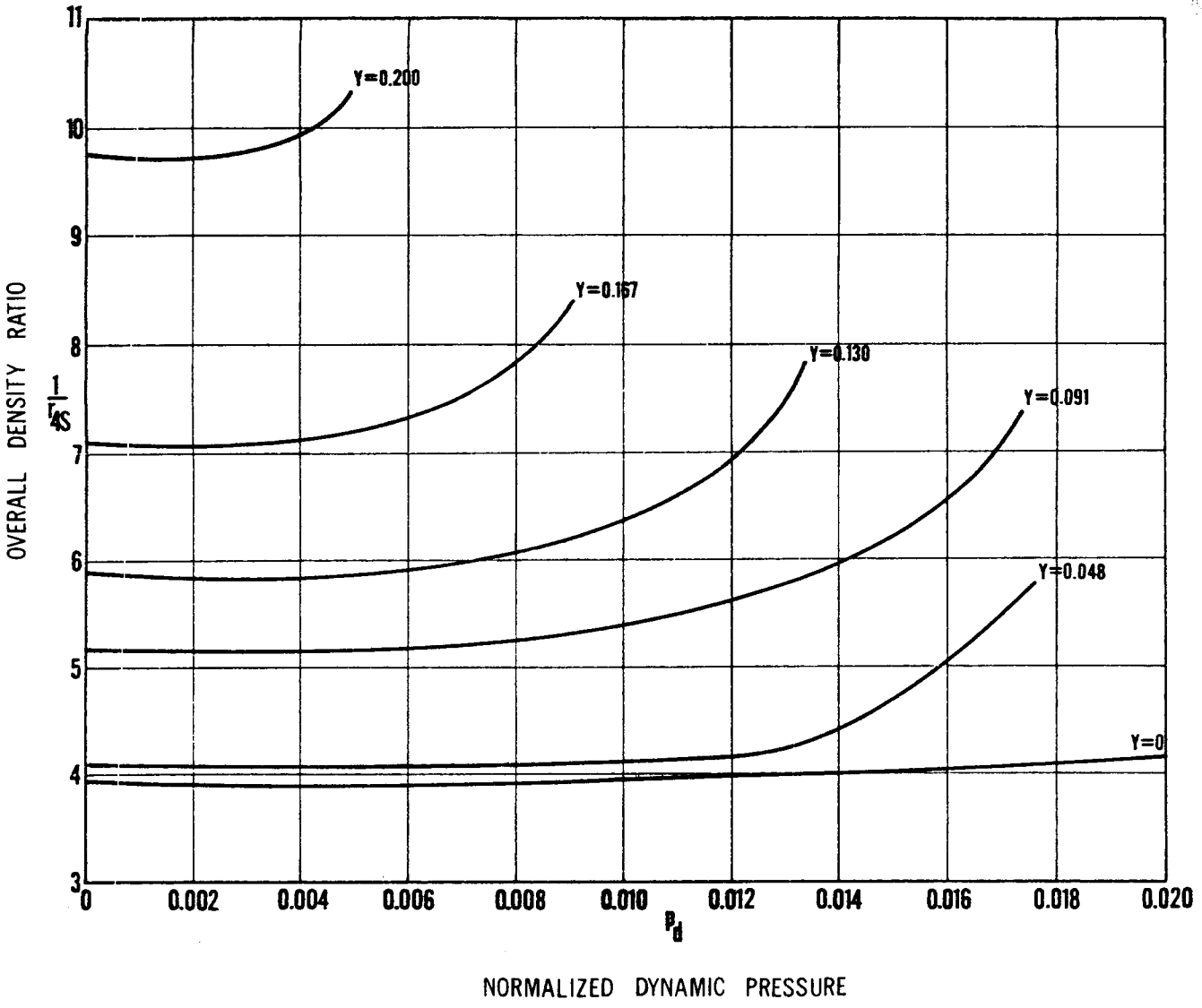

FIG 13.- OVERALL DENSITY RATIO VS NORMALIZED DYNAMIC PRESSURE AT STABILITY BOUNDARY
($l_i = 2.5$, $l_e = 0.5$)

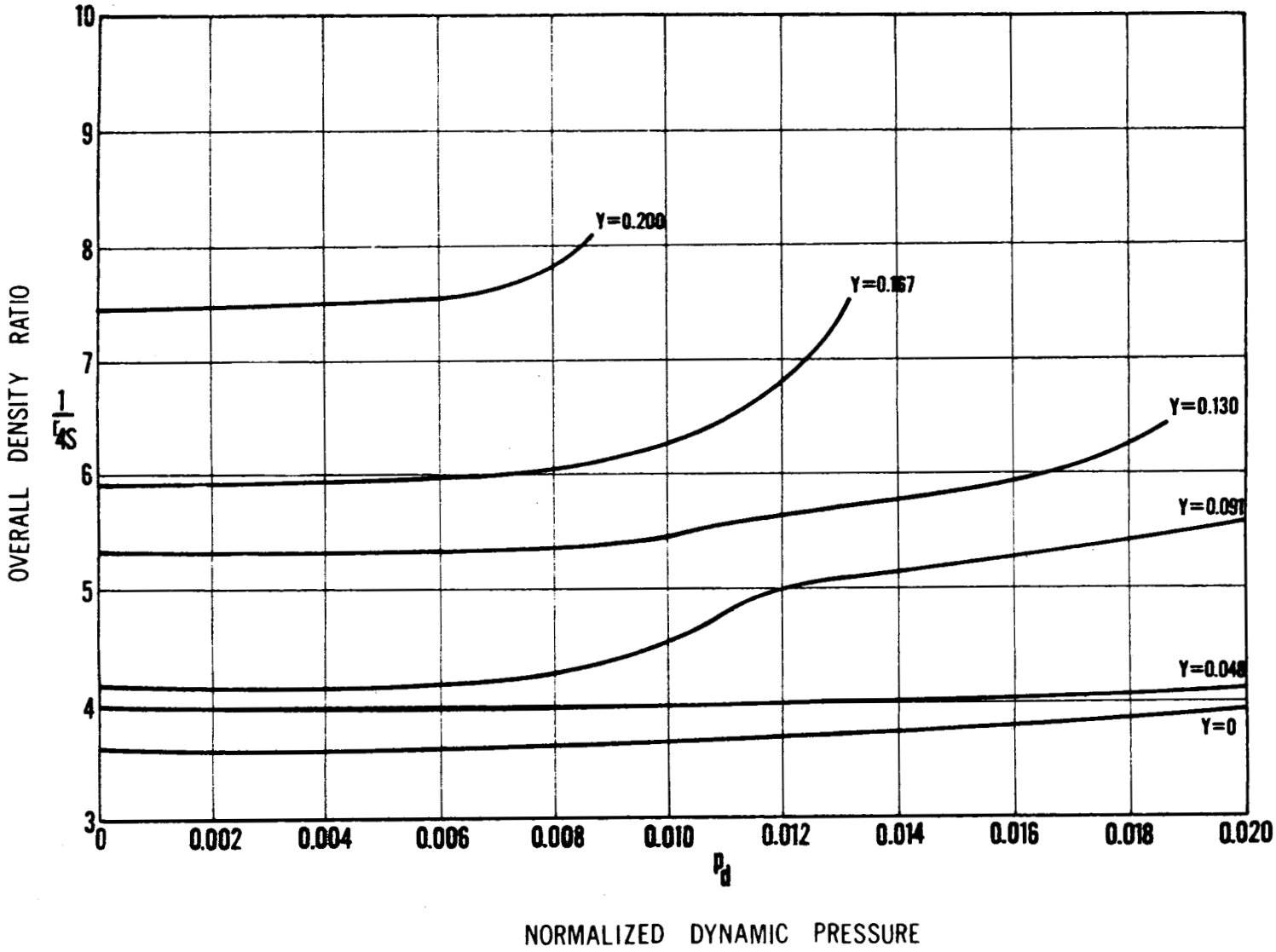

FIG.14.- OVERALL DENSITY RATIO VS NORMALIZED DYNAMIC PRESSURE AT STABILITY BOUNDARY
($l_i = 2.5$, $l_e = 1.0$)

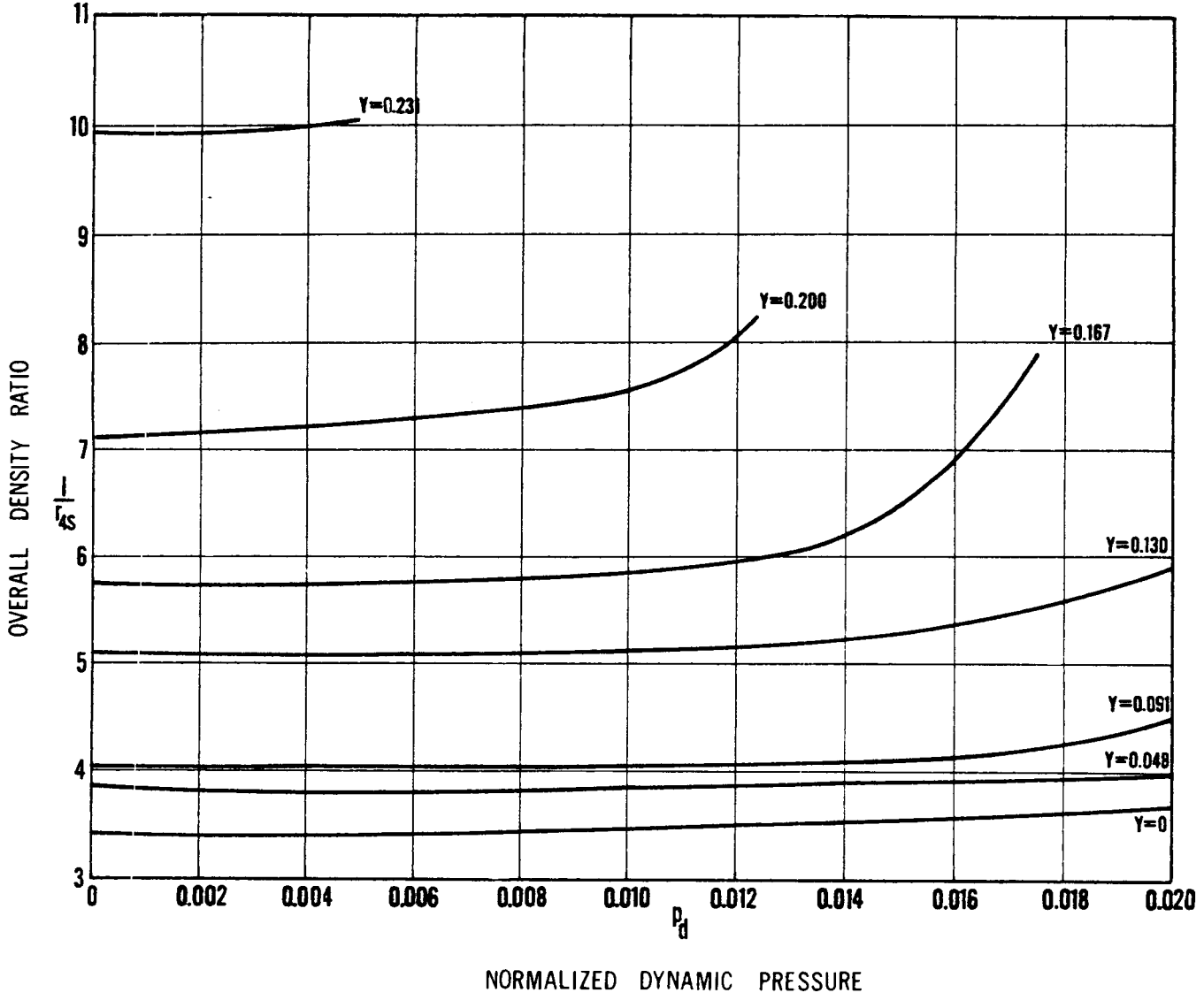

FIG 15.-OVERALL DENSITY RATIO VS NORMALIZED DYNAMIC PRESSURE AT STABILITY BOUNDARY ($l_i = 2.5$, $l_e = 1.5$)

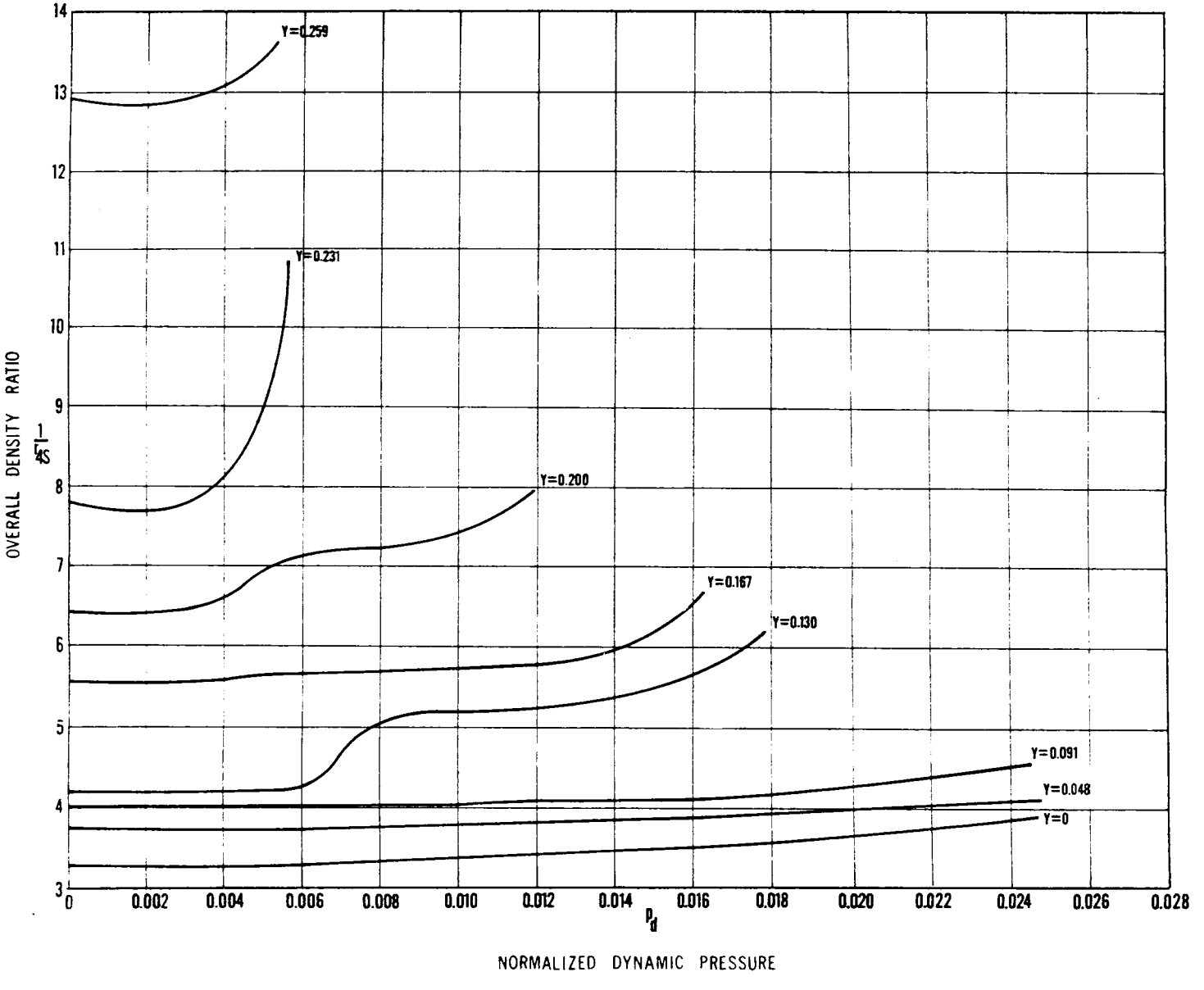

FIG. 16.- OVERALL DENSITY RATIO VS NORMALIZED DYNAMIC PRESSURE AT STABILITY BOUNDARY ($l_i = 3.17, l_e = 2.17$)

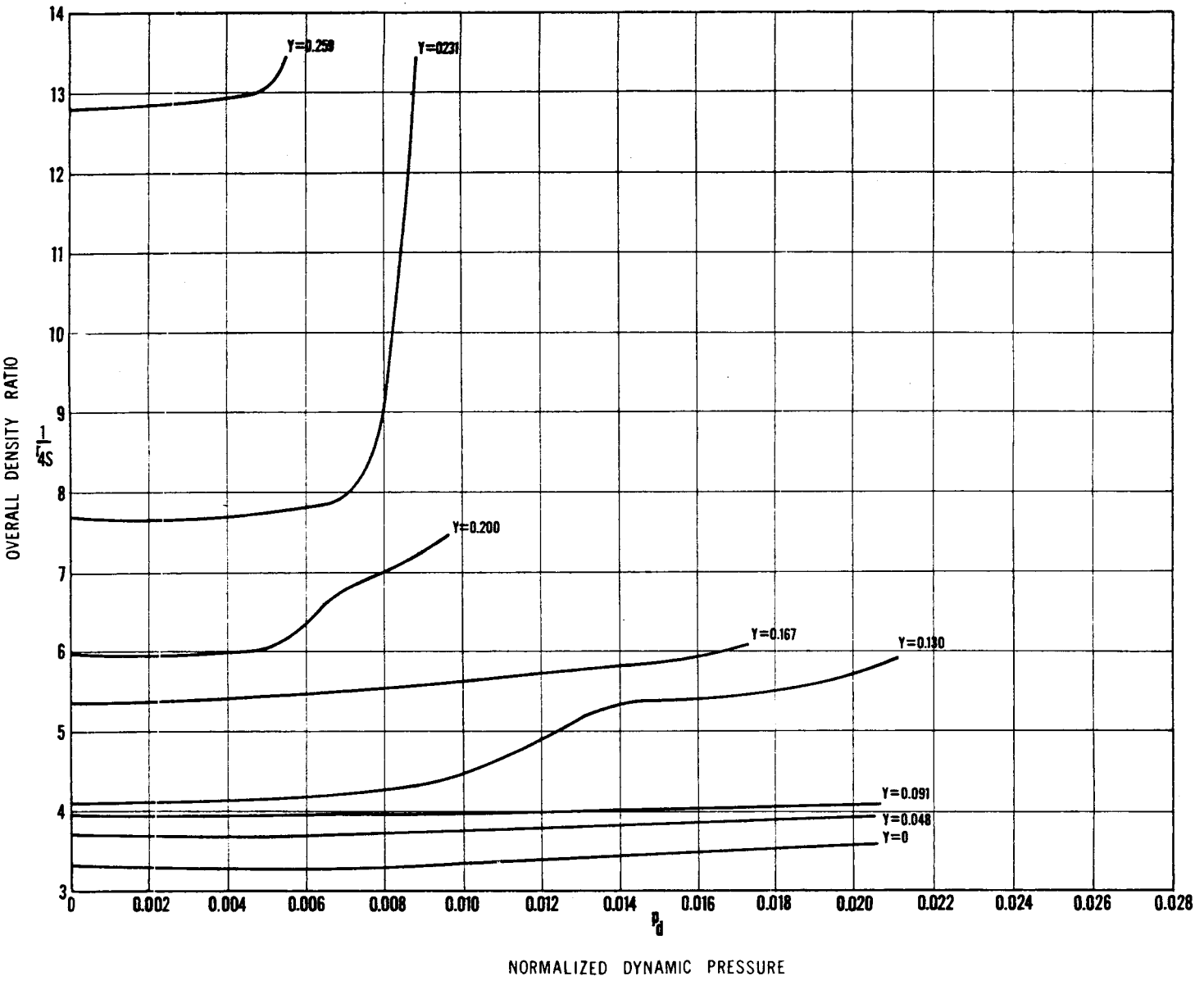

FIG 17.– OVERALL DENSITY RATIO VS NORMALIZED DYNAMIC PRESSURE AT STABILITY BOUNDARY ($I_i = 3.67$, $I_e = 2.67$)

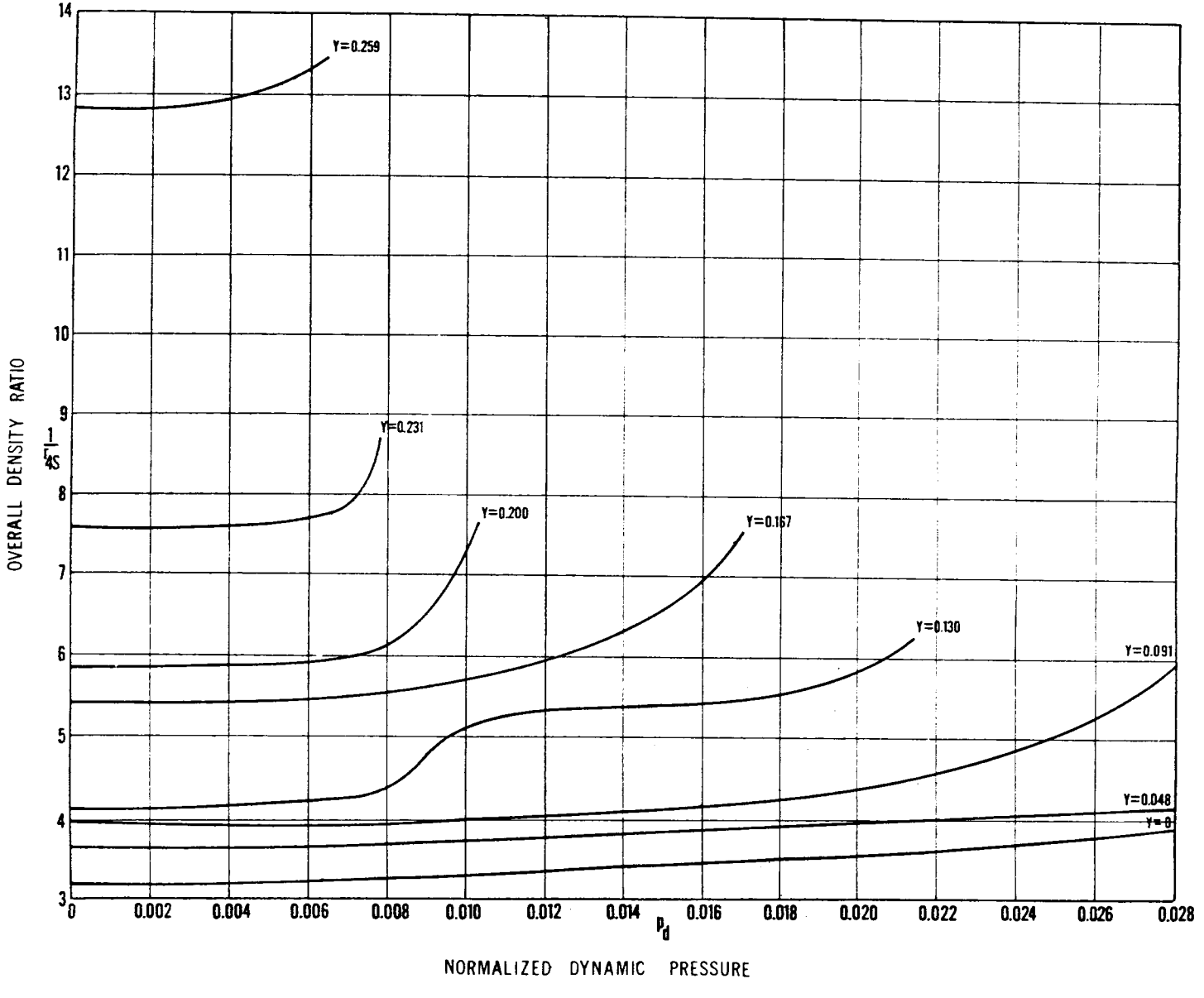

FIG. 18.- OVERALL DENSITY RATIO VS NORMALIZED DYNAMIC PRESSURE AT STABILITY BOUNDARY (l_i=4.5, l_e=3.5)

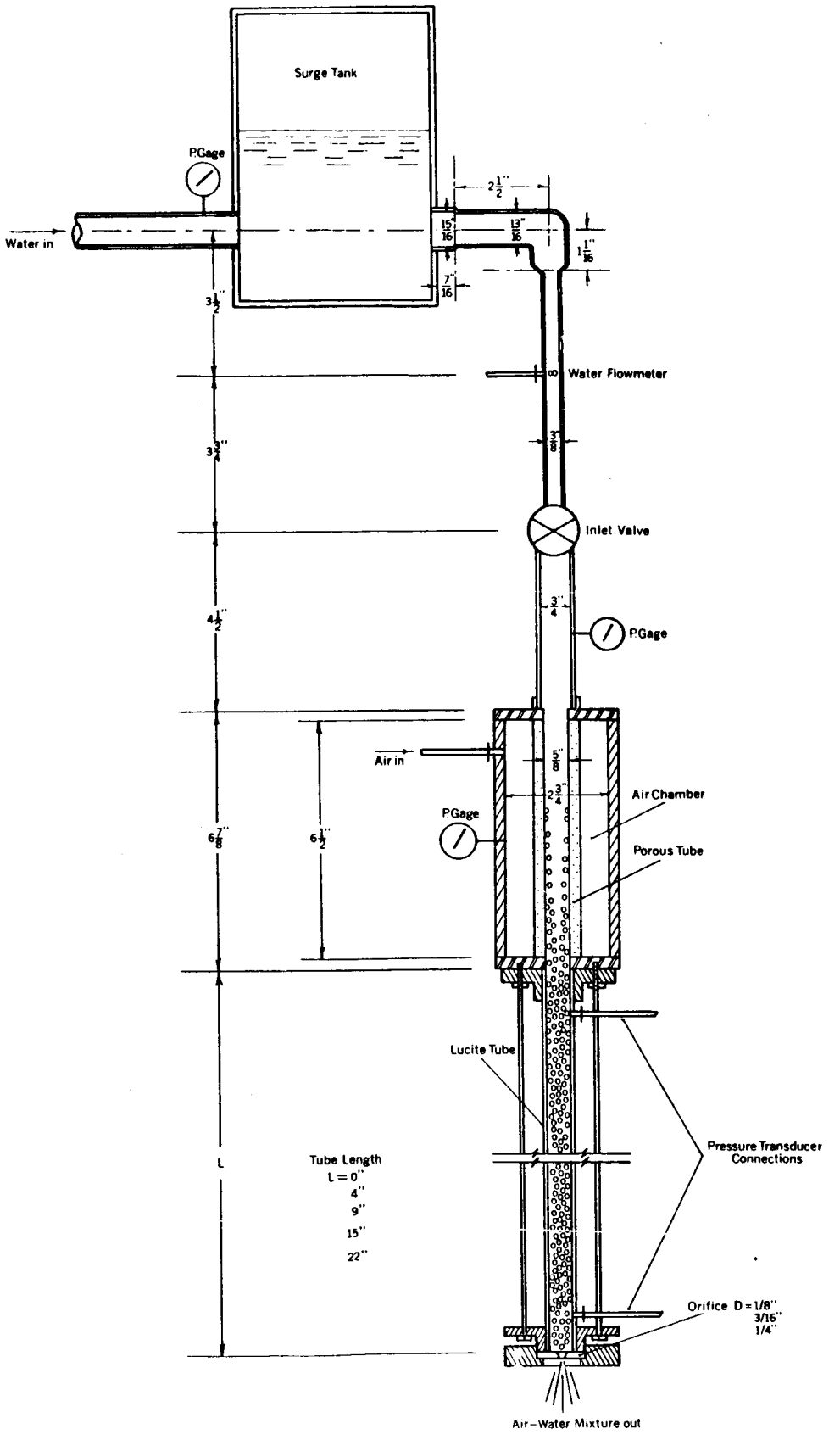

FIG. 19 - AIR-WATER APPARATUS TEST SECTION

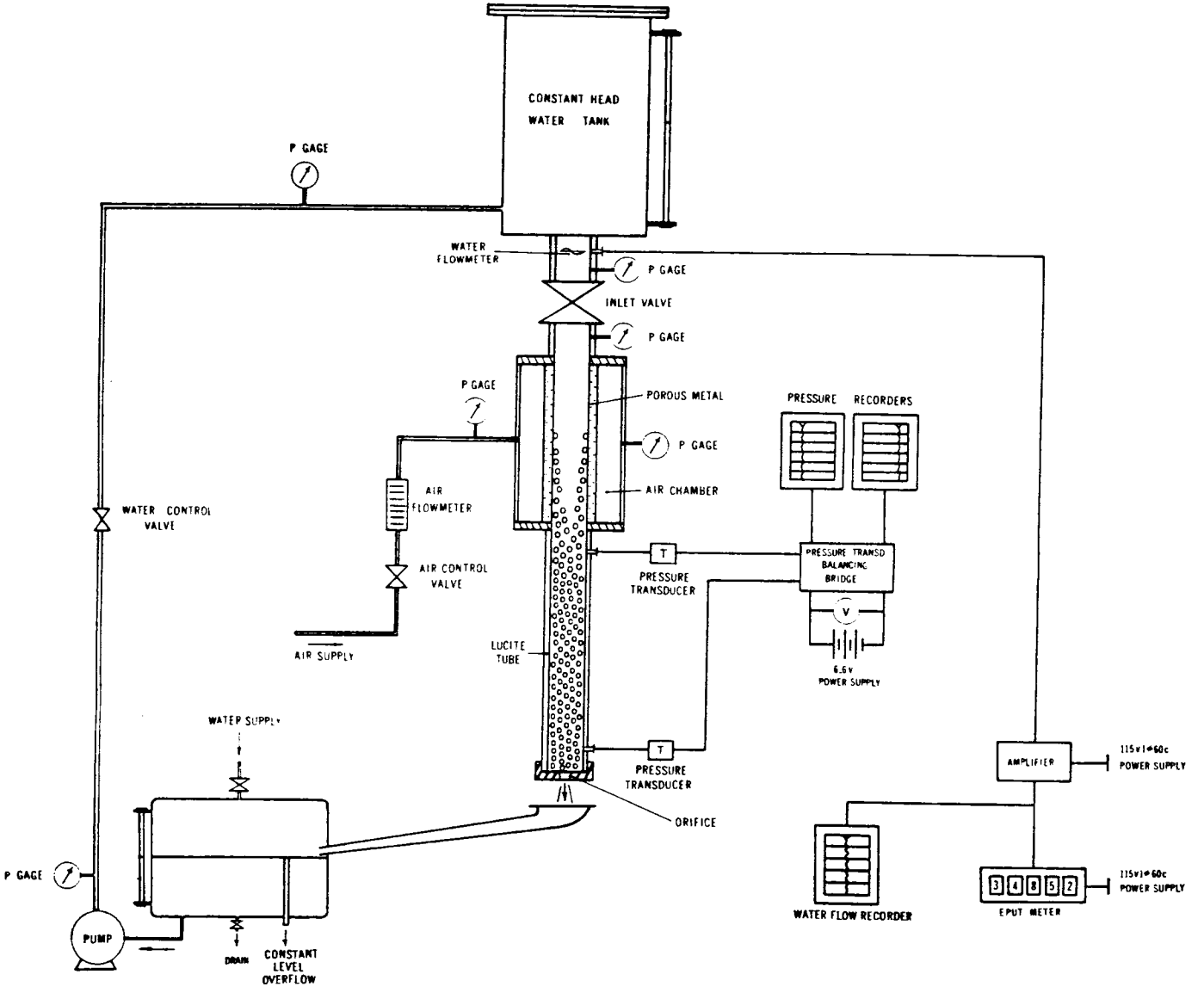

FIGURE 20.–SCHEMATIC DIAGRAM OF EXPERIMENTAL SET-UP FOR TWO-PHASE INSTABILITY [AIR-WATER APPARATUS]

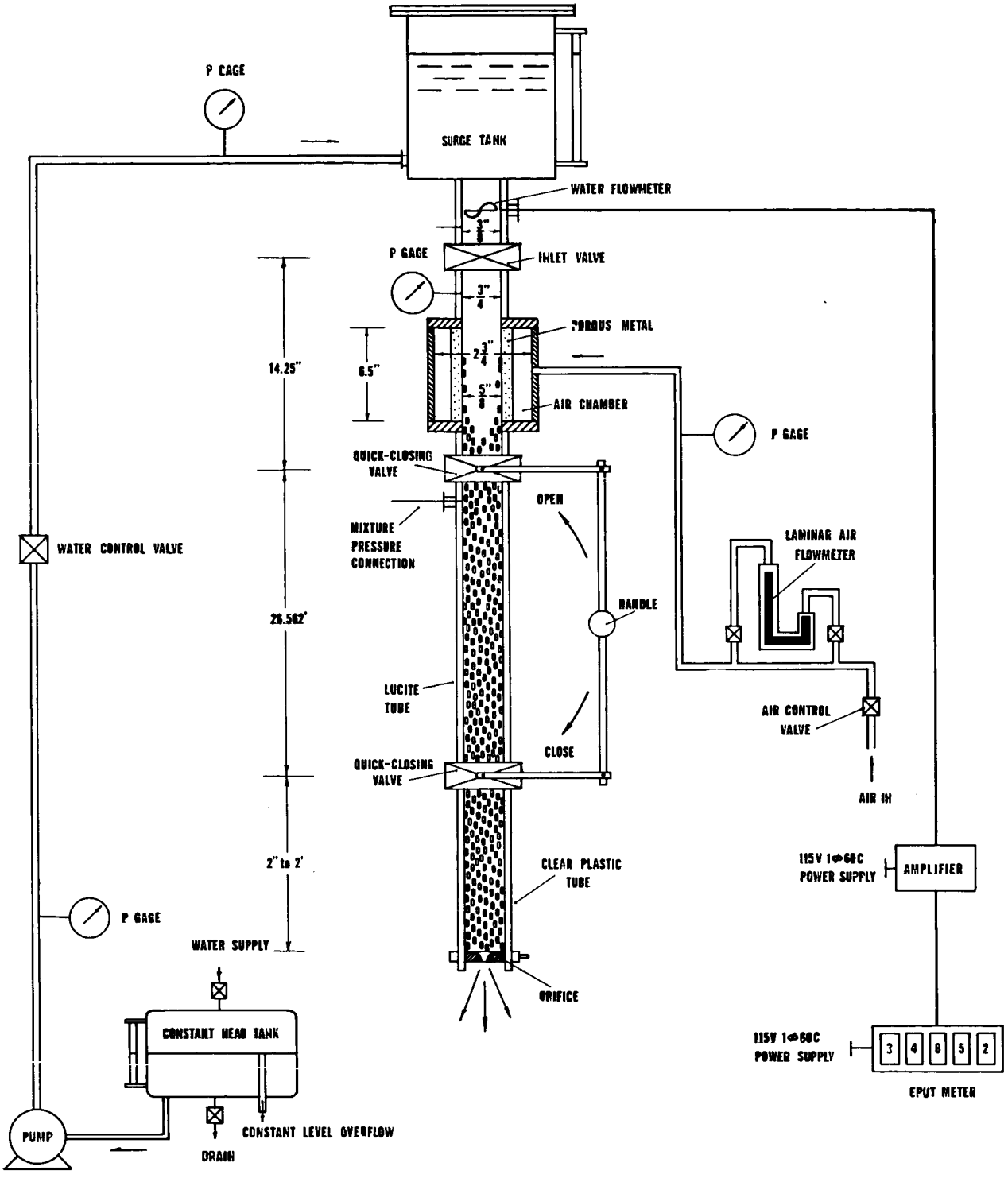

FIG.21. - SCHEMATIC DIAGRAM OF EXPERIMENTAL SET-UP FOR SLIP INVESTIGATION

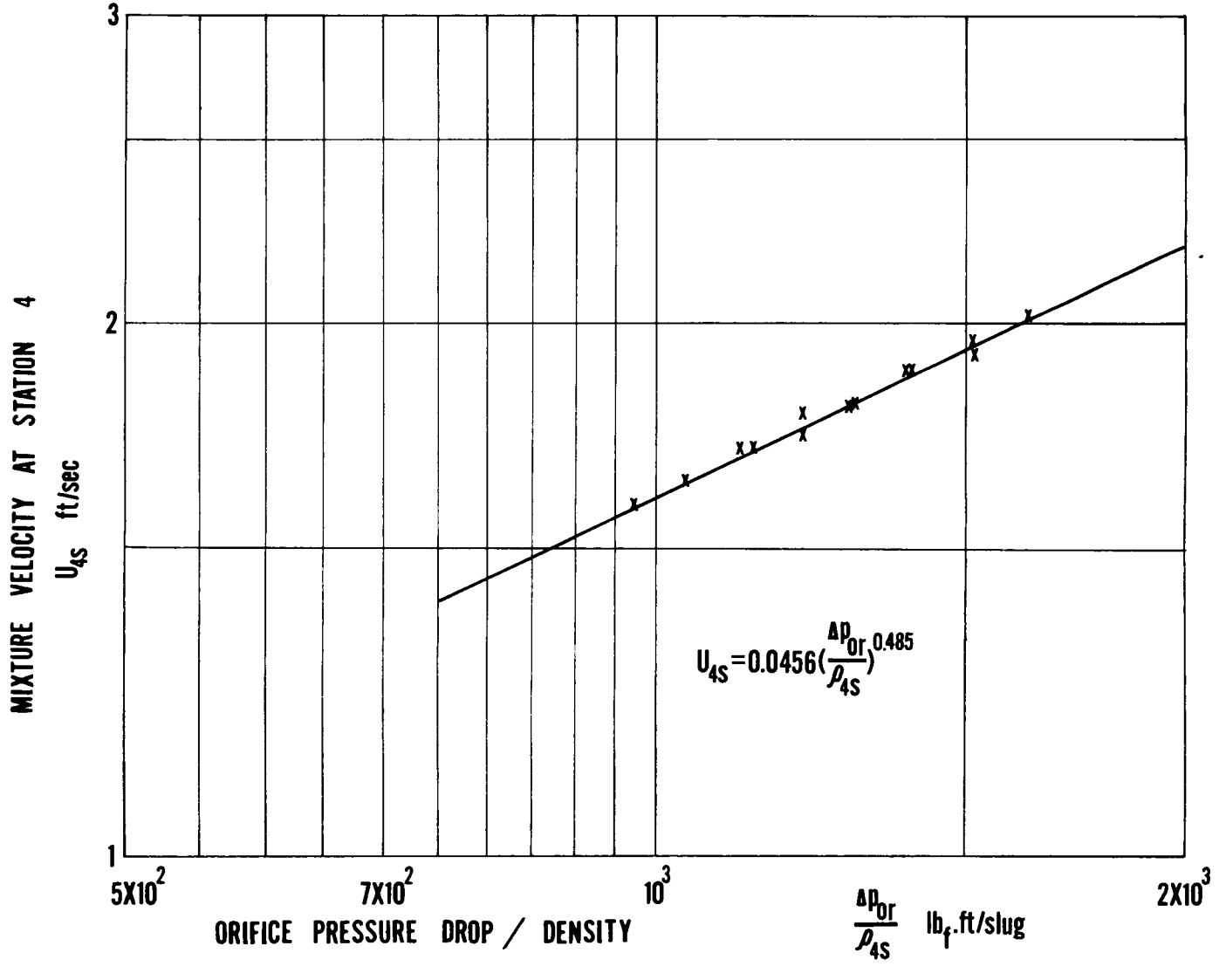

FIG.22.– 1/8" DIA. ORIFICE CALIBRATION FOR TWO-PHASE FLOW

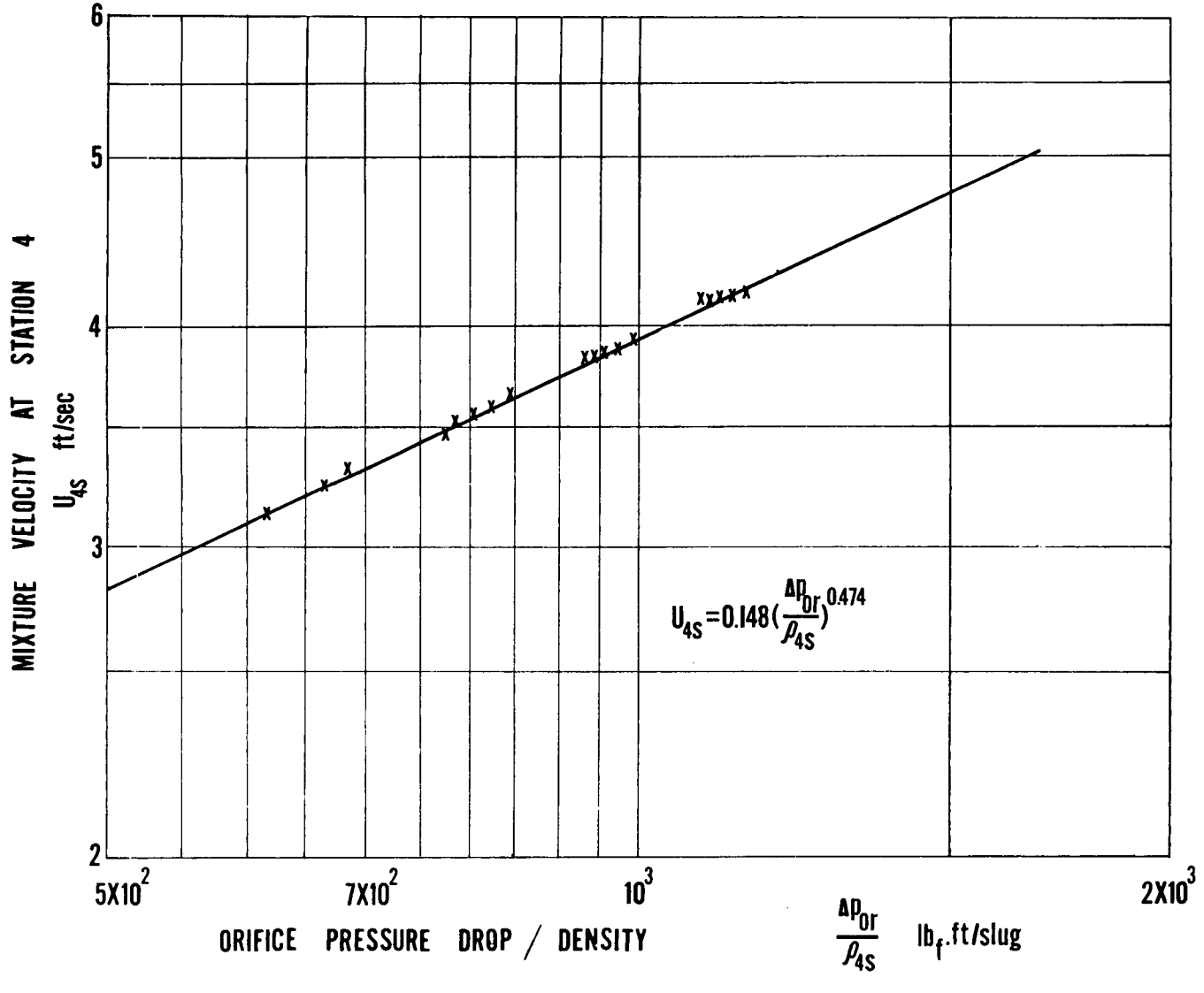

FIG.23.– 3/16" DIA. ORIFICE CALIBRATION FOR TWO-PHASE FLOW

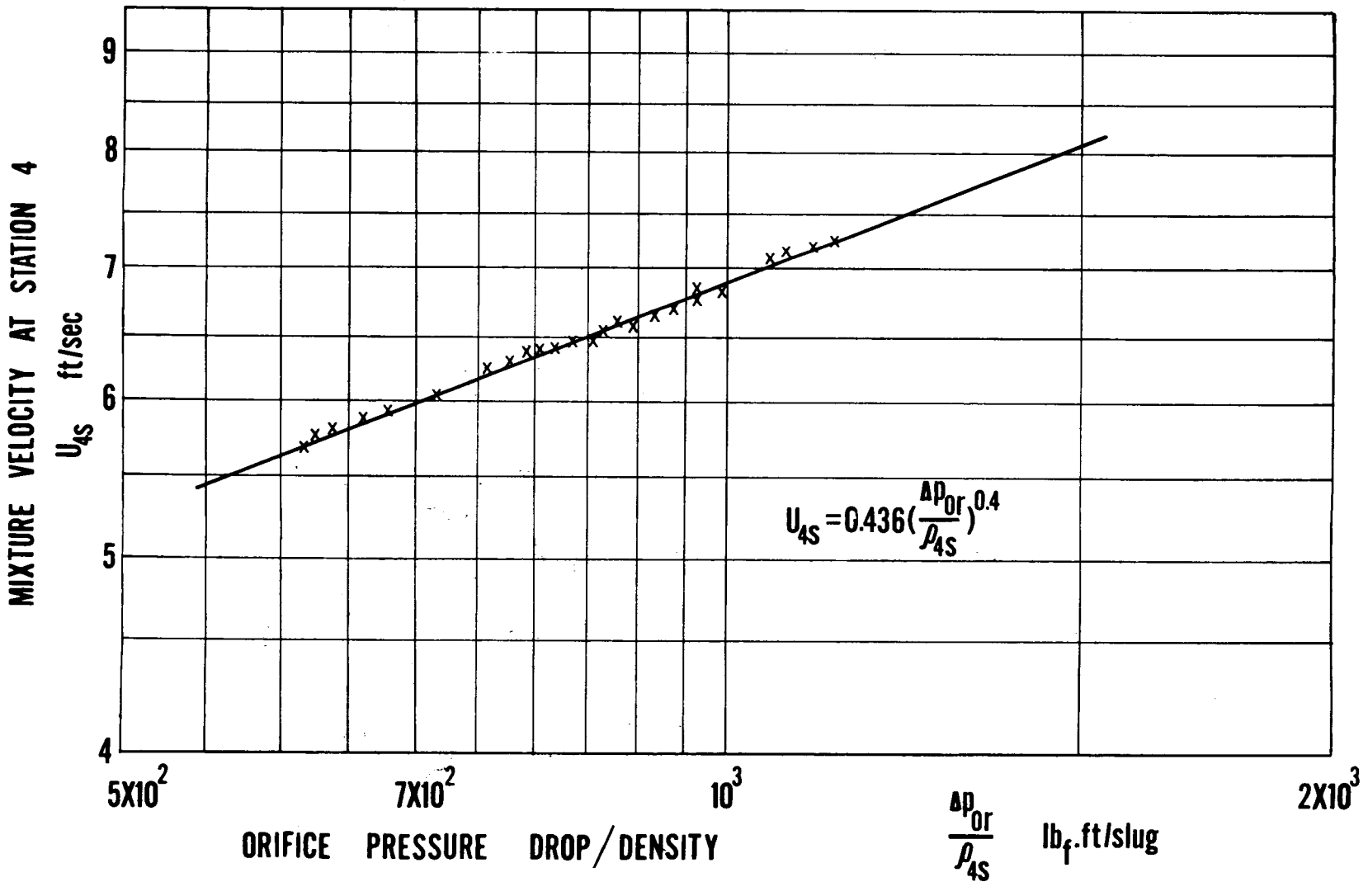

FIG.24.—1/4" DIA. ORIFICE CALIBRATION FOR TWO-PHASE FLOW

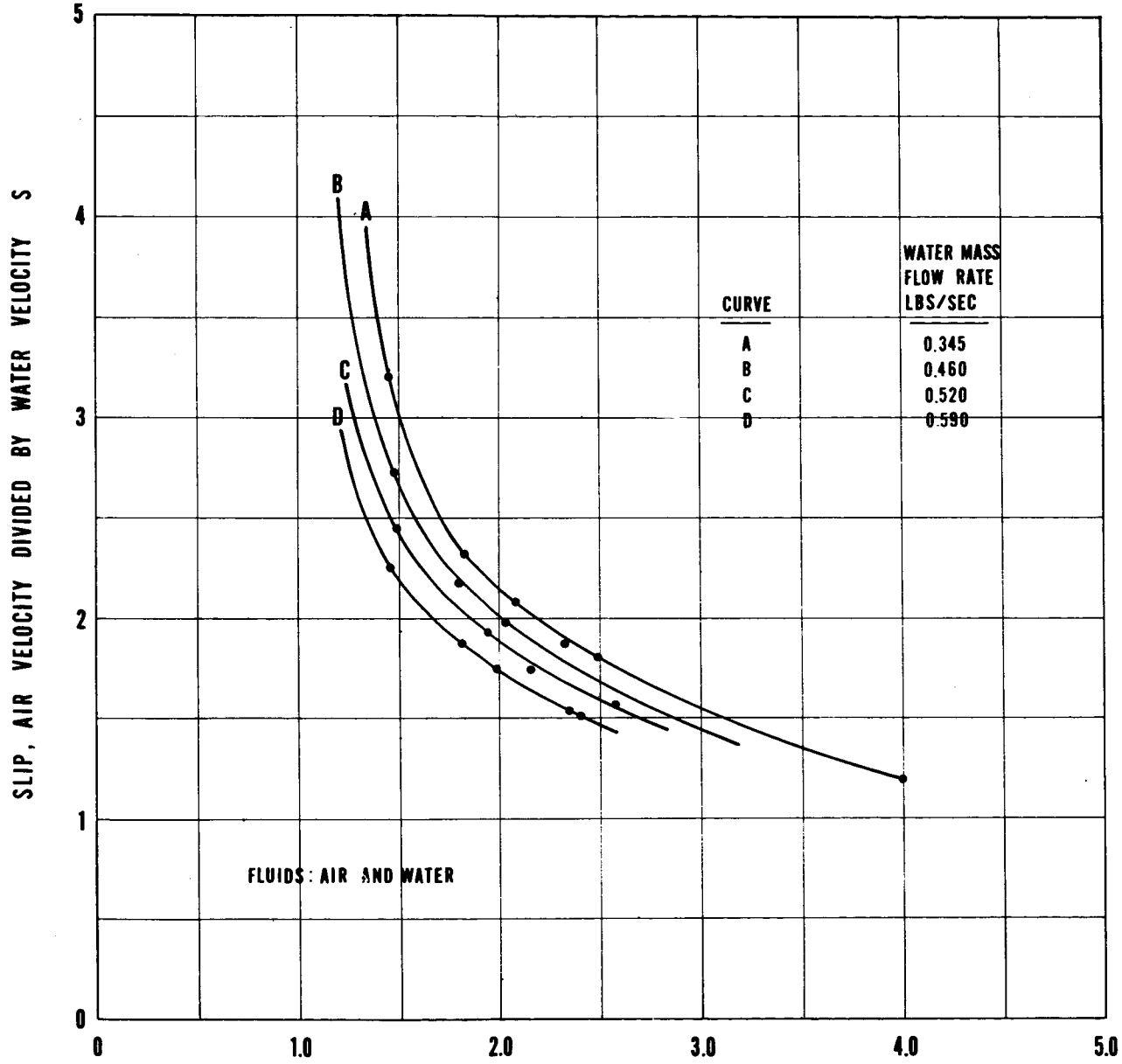

FIG.25.– SLIP VS DENSITY RATIO

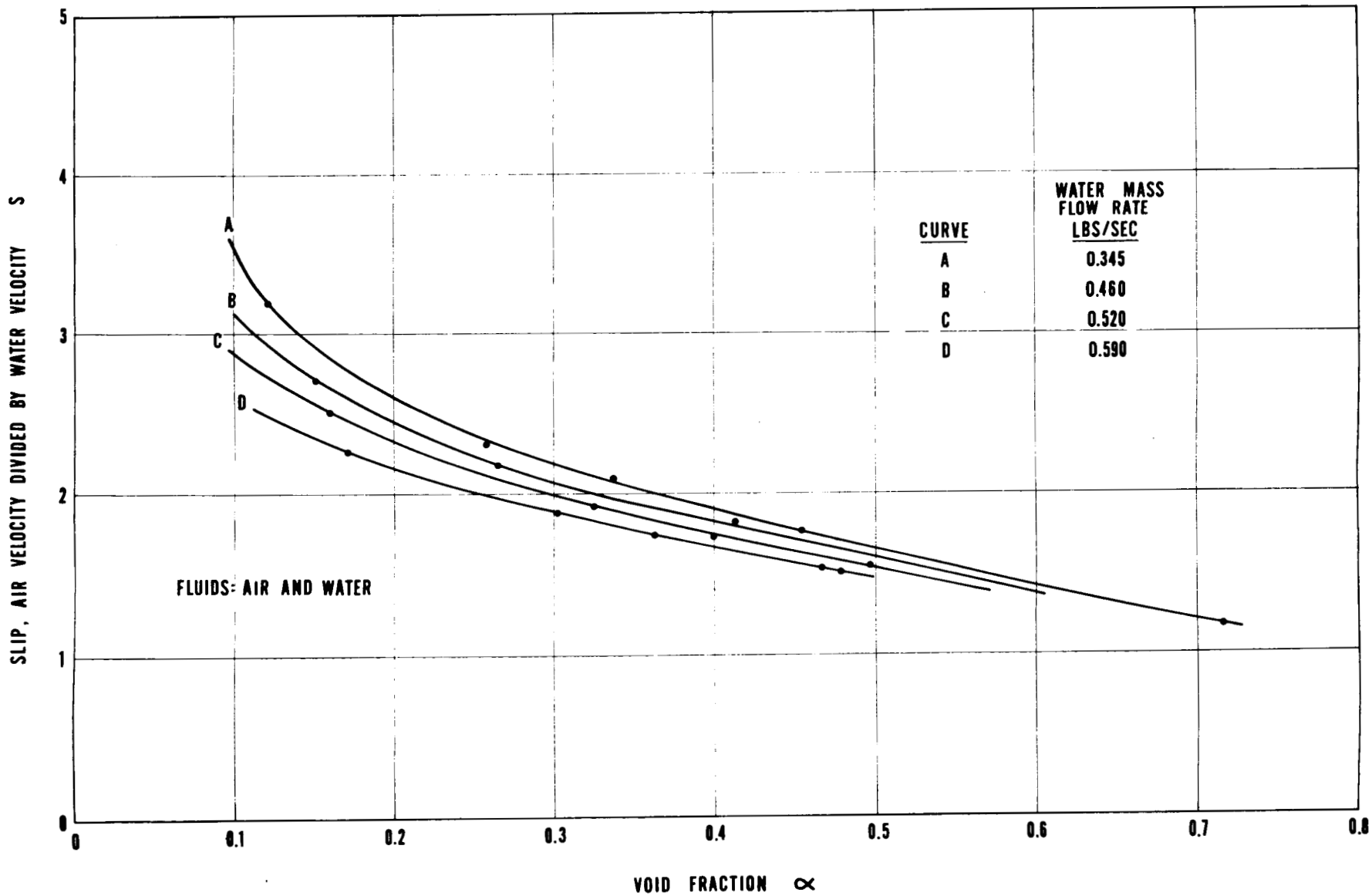

FIG.26.– SLIP VS VOID FRACTION

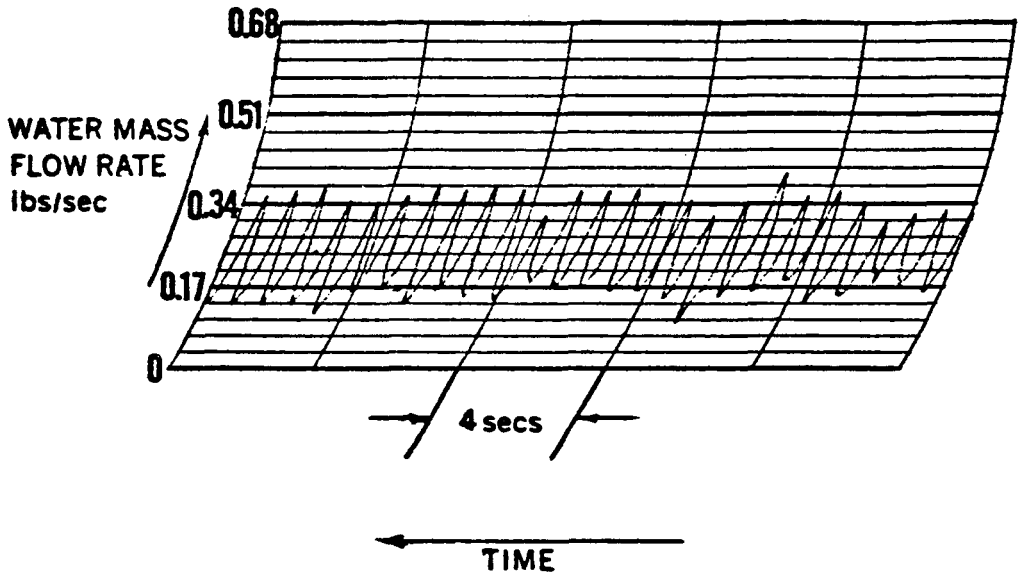

FIG.27.— A RECORDING OF WATER MASS FLOW RATE OSCILLATIONS NEAR STABILITY BOUNDARY

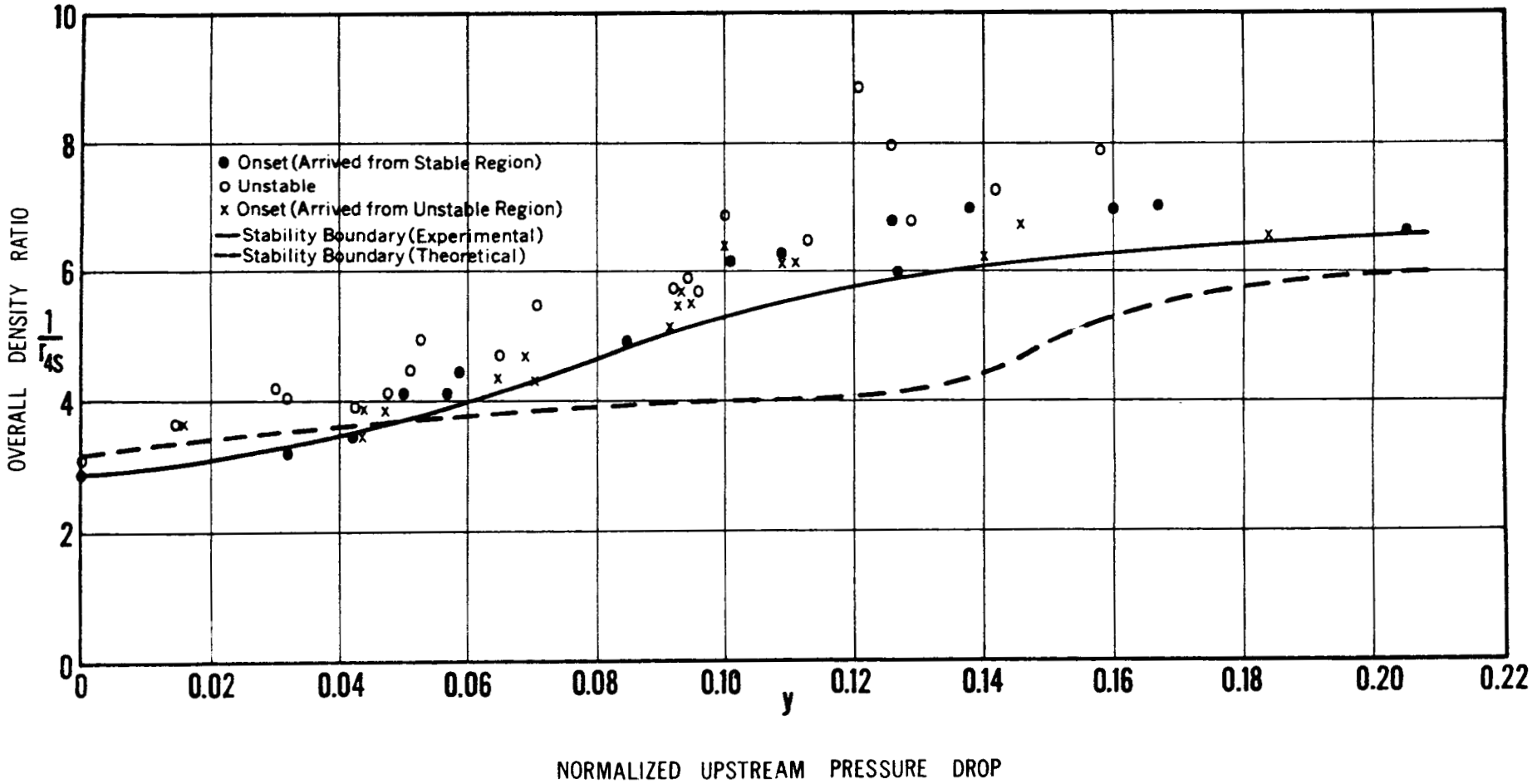

FIG.28.– EXPERIMENTAL AND THEORETICAL STABILITY BOUNDARY (L_e=22 in., D_{or}=1/8 in)

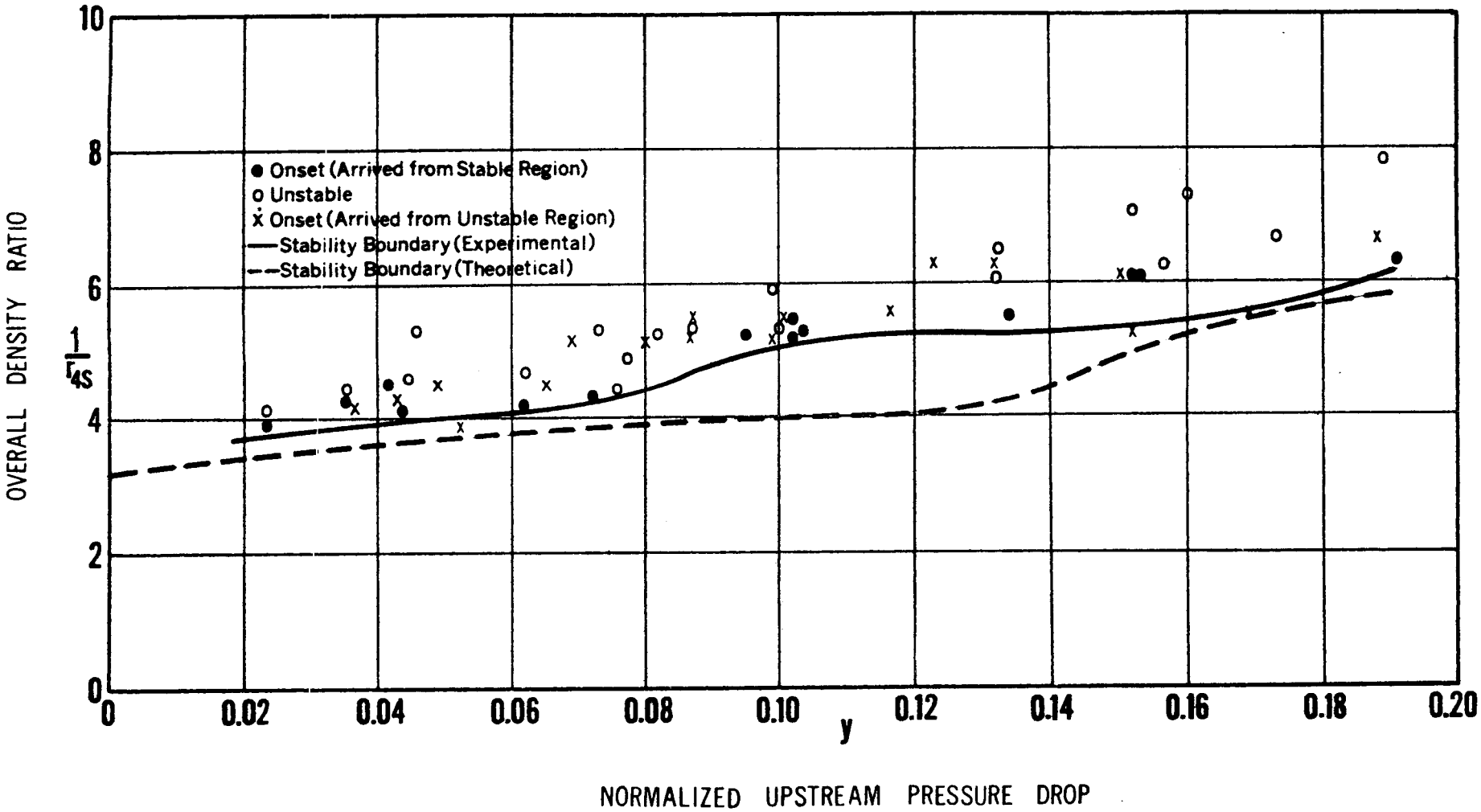

FIG.29.– EXPERIMENTAL AND THEORETICAL STABILITY BOUNDARY ($L_e = 22$ in., $D_{or} = 3/16$ in.)

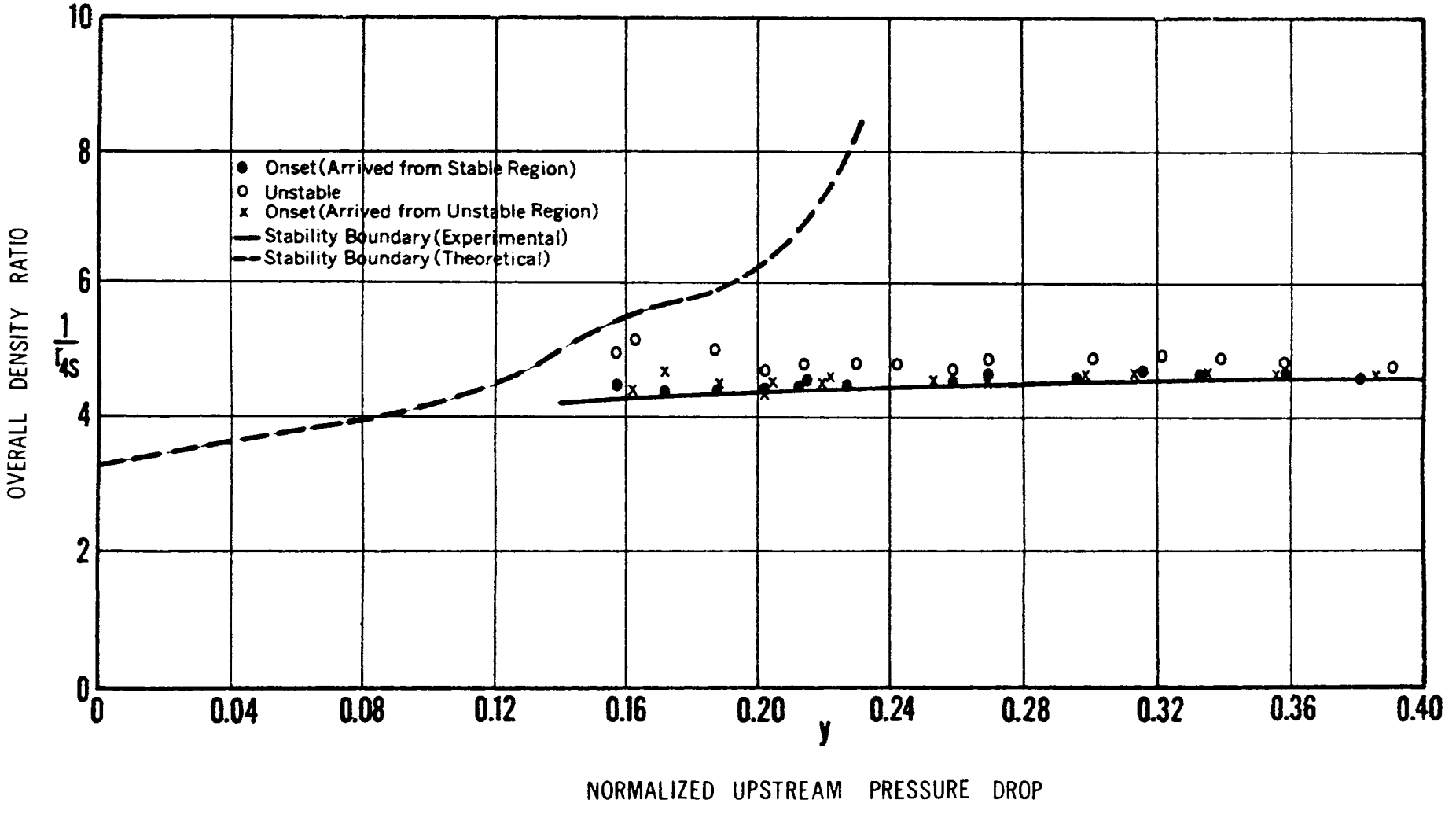

FIG. 30. – EXPERIMENTAL AND THEORETICAL STABILITY BOUNDARY (L_e = 22 in., D_{or} = 1/4 in.)

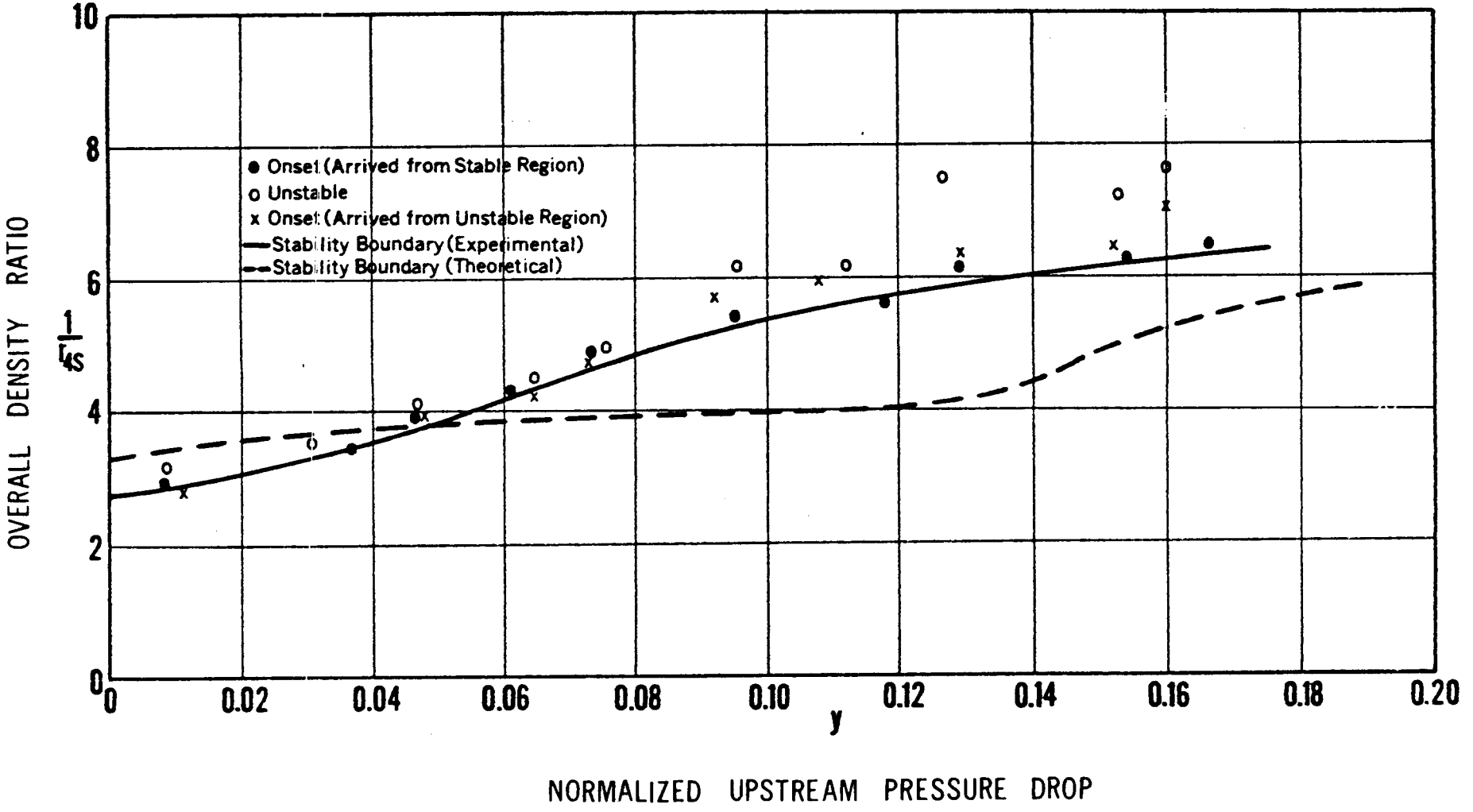

FIG.31.– EXPERIMENTAL AND THEORETICAL STABILITY BOUNDARY (L_e=15 in., D_{or}=1/8 in.)

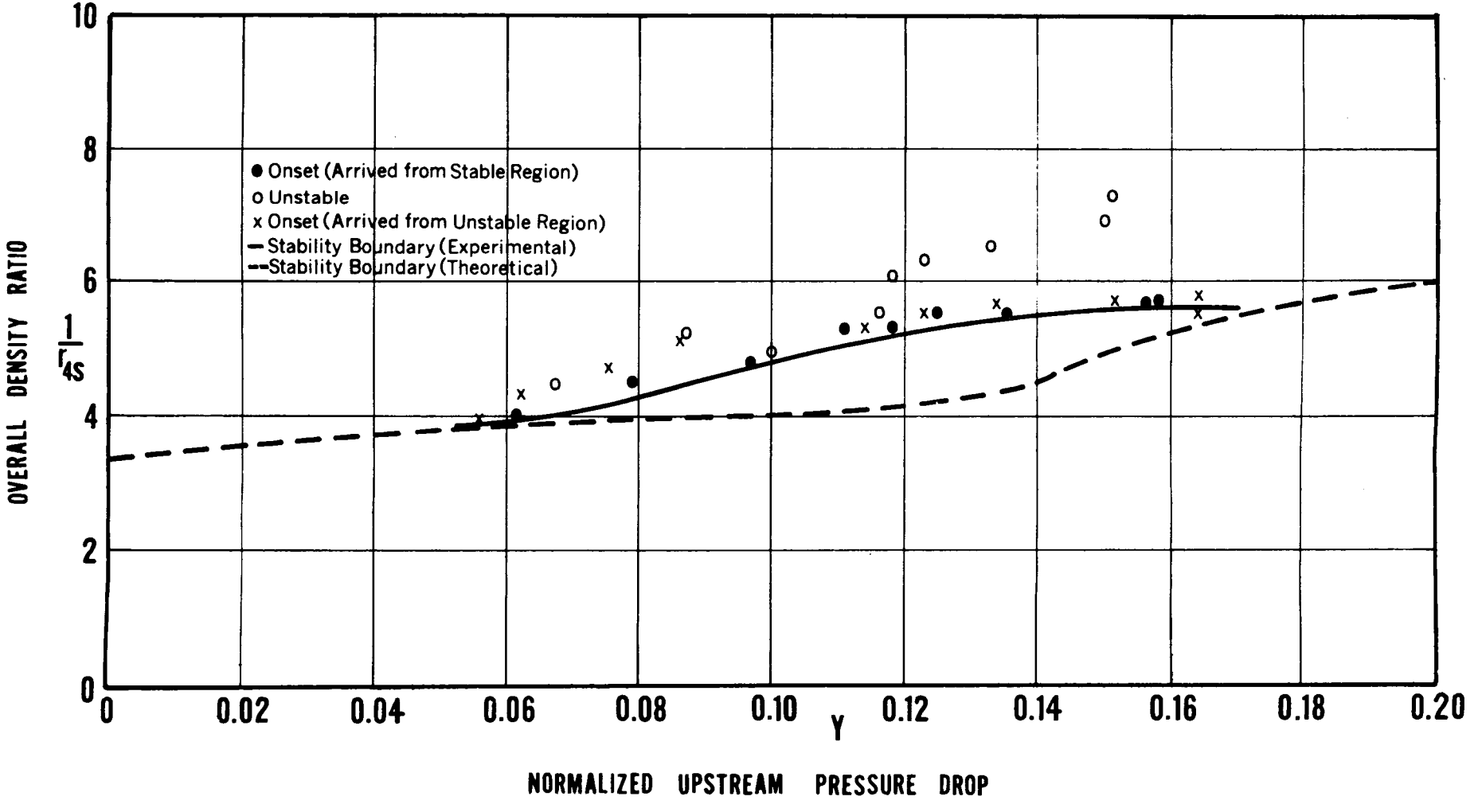

FIG. 32. – EXPERIMENTAL AND THEORETICAL STABILITY BOUNDARY (L_e = 15 in., D_{or} = 3/16 in.)

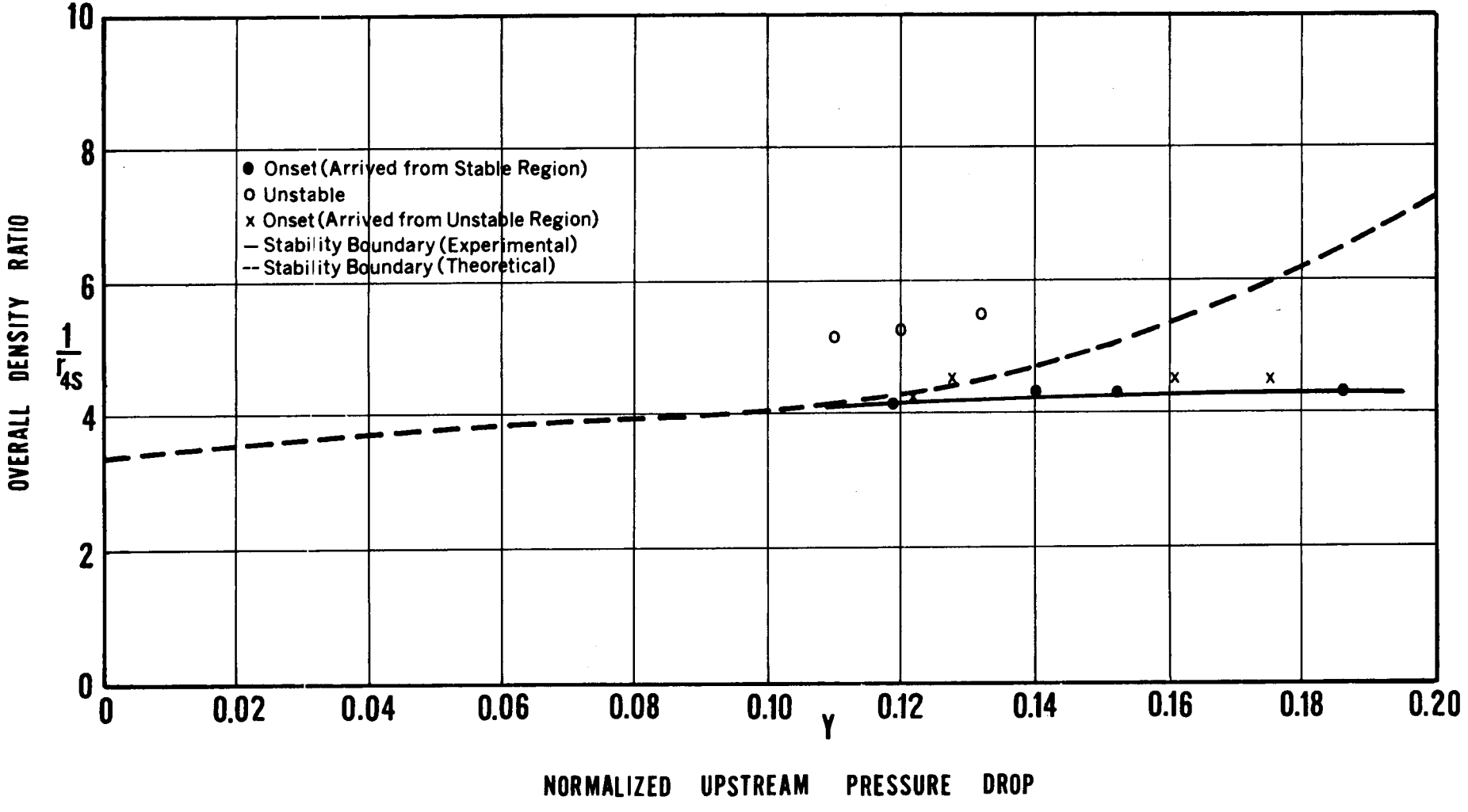

FIG. 33. – EXPERIMENTAL AND THEORETICAL STABILITY BOUNDARY (L_e=15in., D_{or}=1/4in.)

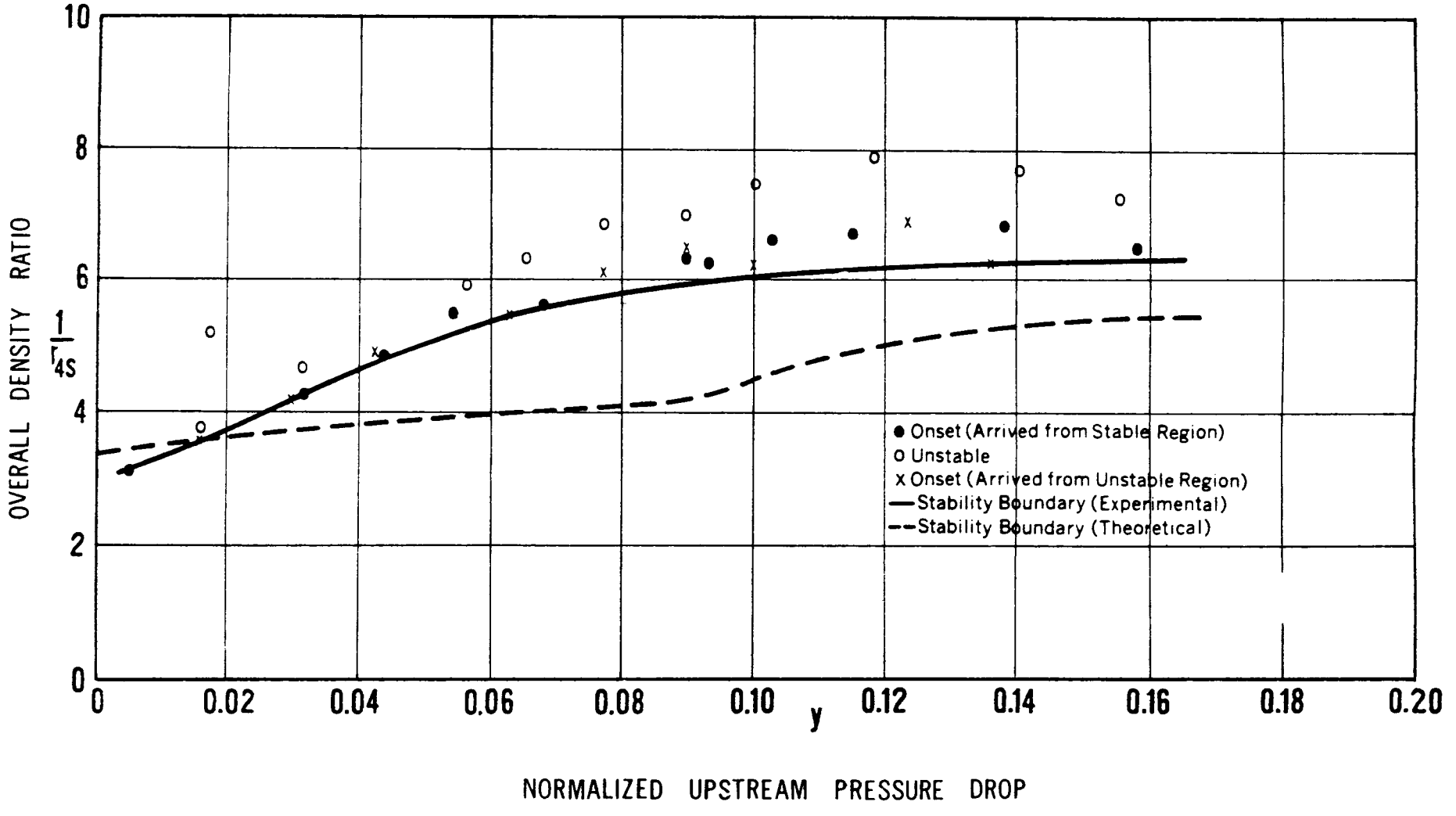

FIG.34.- EXPERIMENTAL AND THEORETICAL STABILITY BOUNDARY (L_e = 9 in., D_{or} = 1/8 in.)

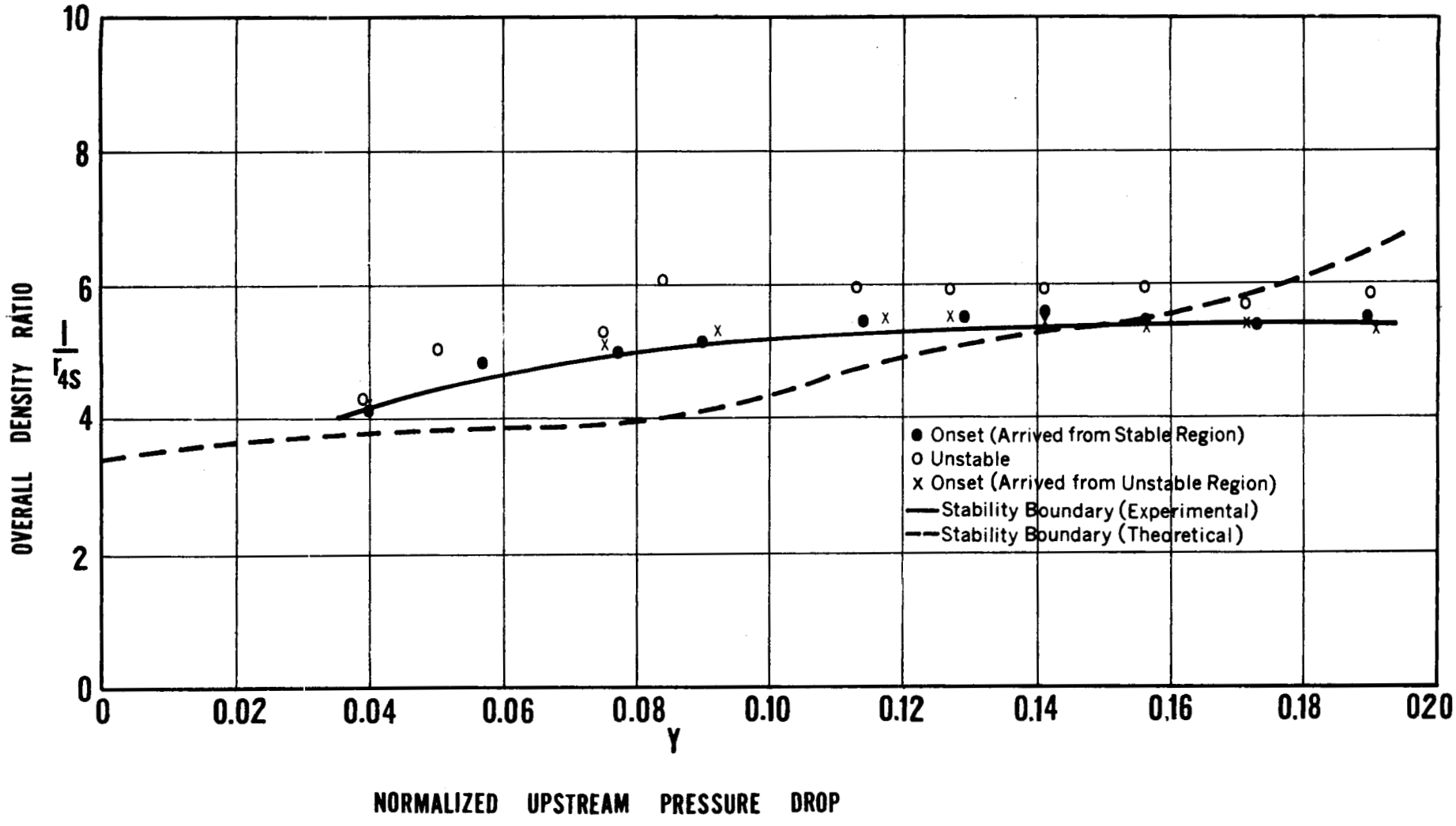

FIG. 35.– EXPERIMENTAL AND THEORETICAL STABILITY BOUNDARY (L_e = 9 in., D_{or} = 3/16 in.)

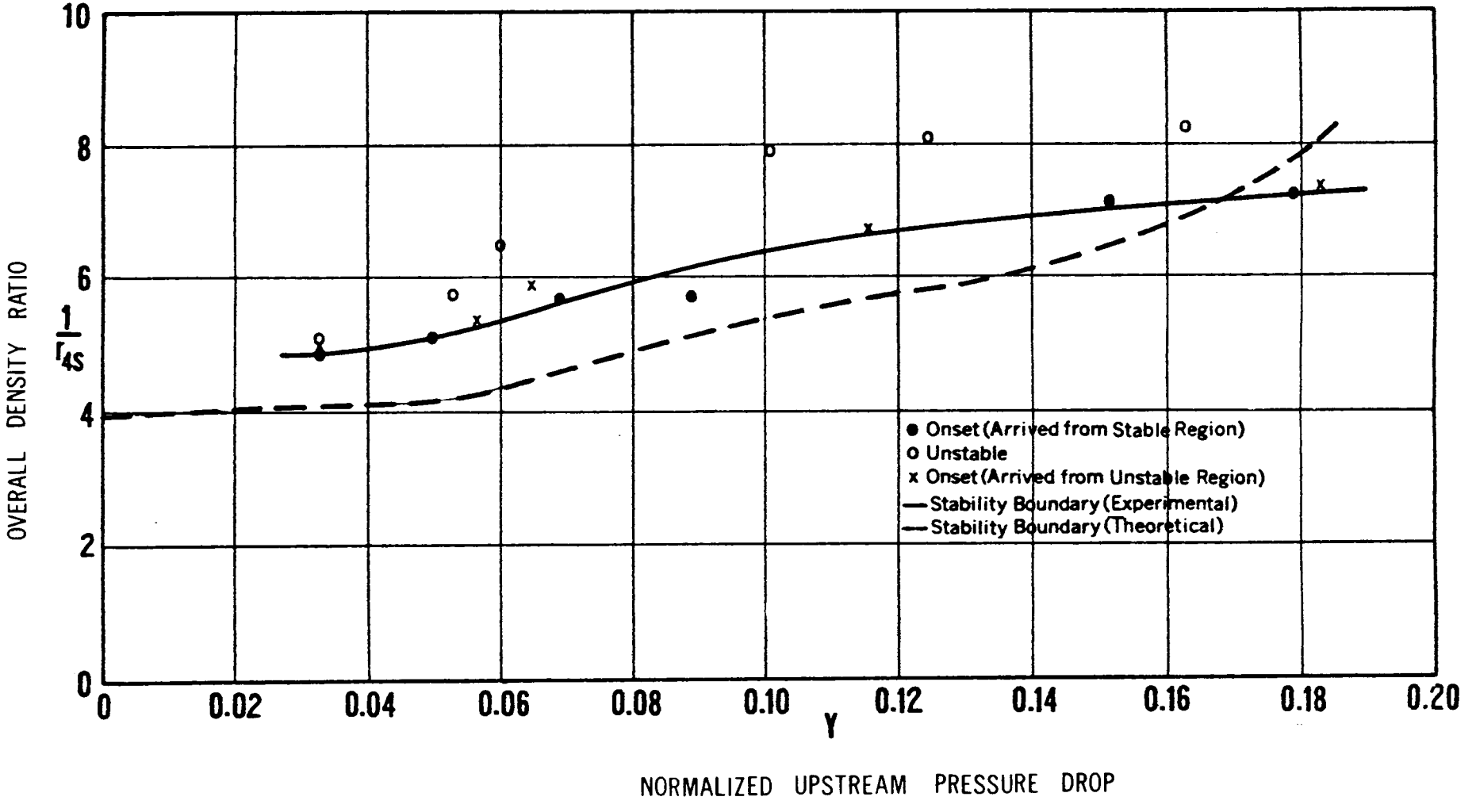

FIG. 36. – EXPERIMENTAL AND THEORETICAL STABILITY BOUNDARY ($L_e = 4$ in., $D_{or} = 1/8$ in.)

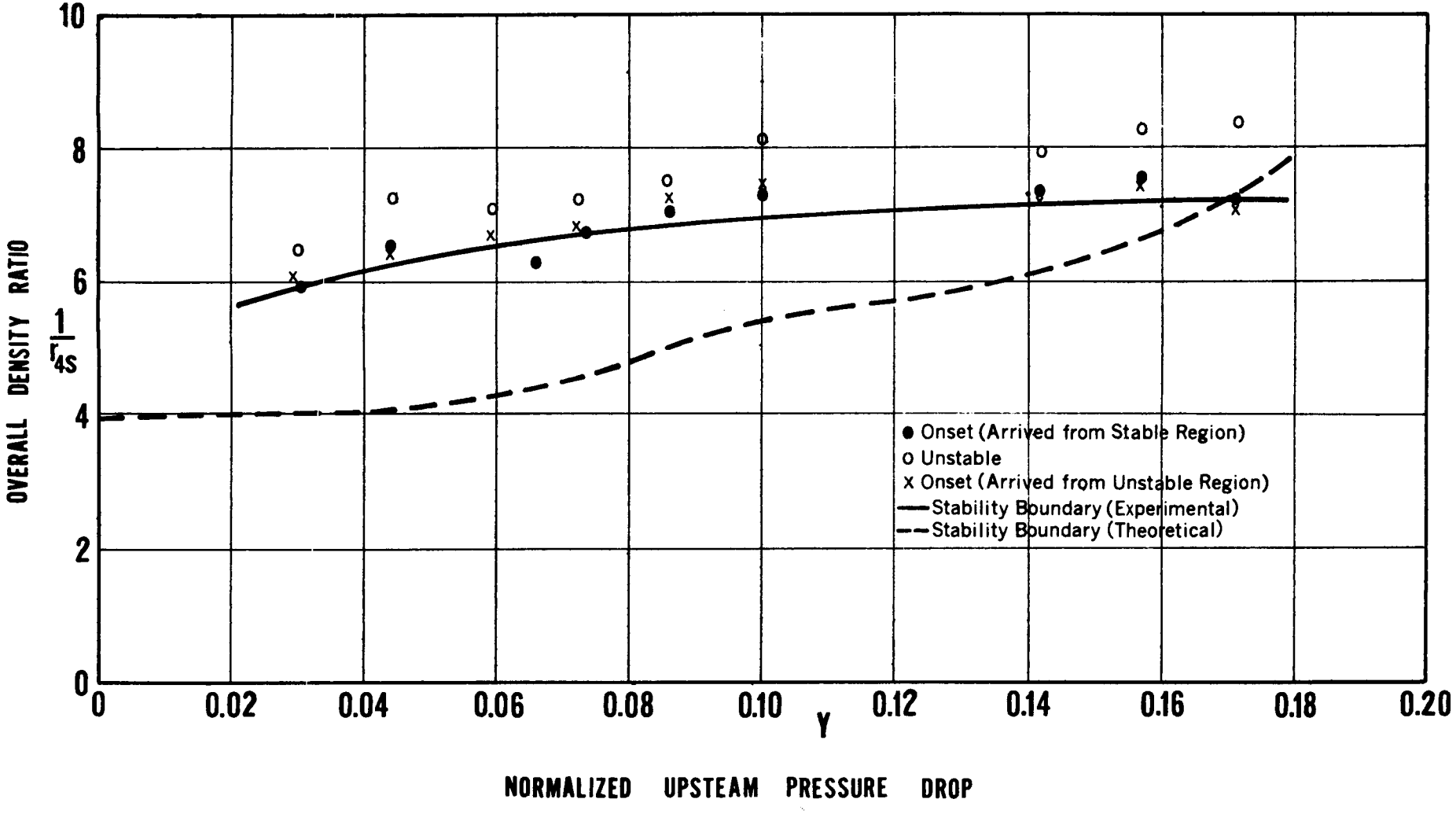

FIG. 37.– EXPERIMENTAL AND THEORETICAL STABILITY BOUNDARY (L_e=4in., D_{or}=3/16in.)

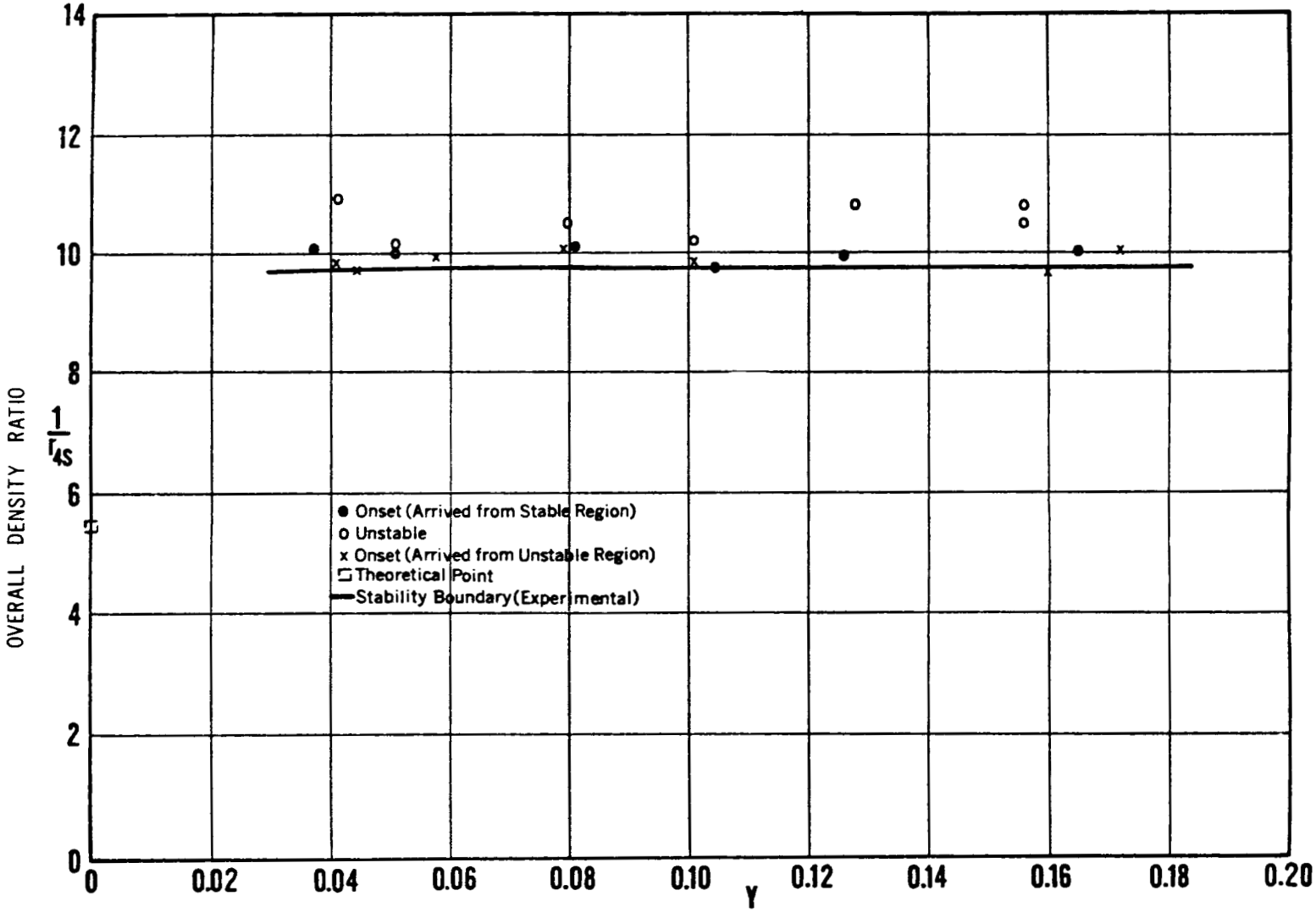

FIG. 38 – EXPERIMENTAL AND THEORETICAL STABILITY BOUNDARY ($L_e = 0$, $D_{or} = 1/8$ in.)

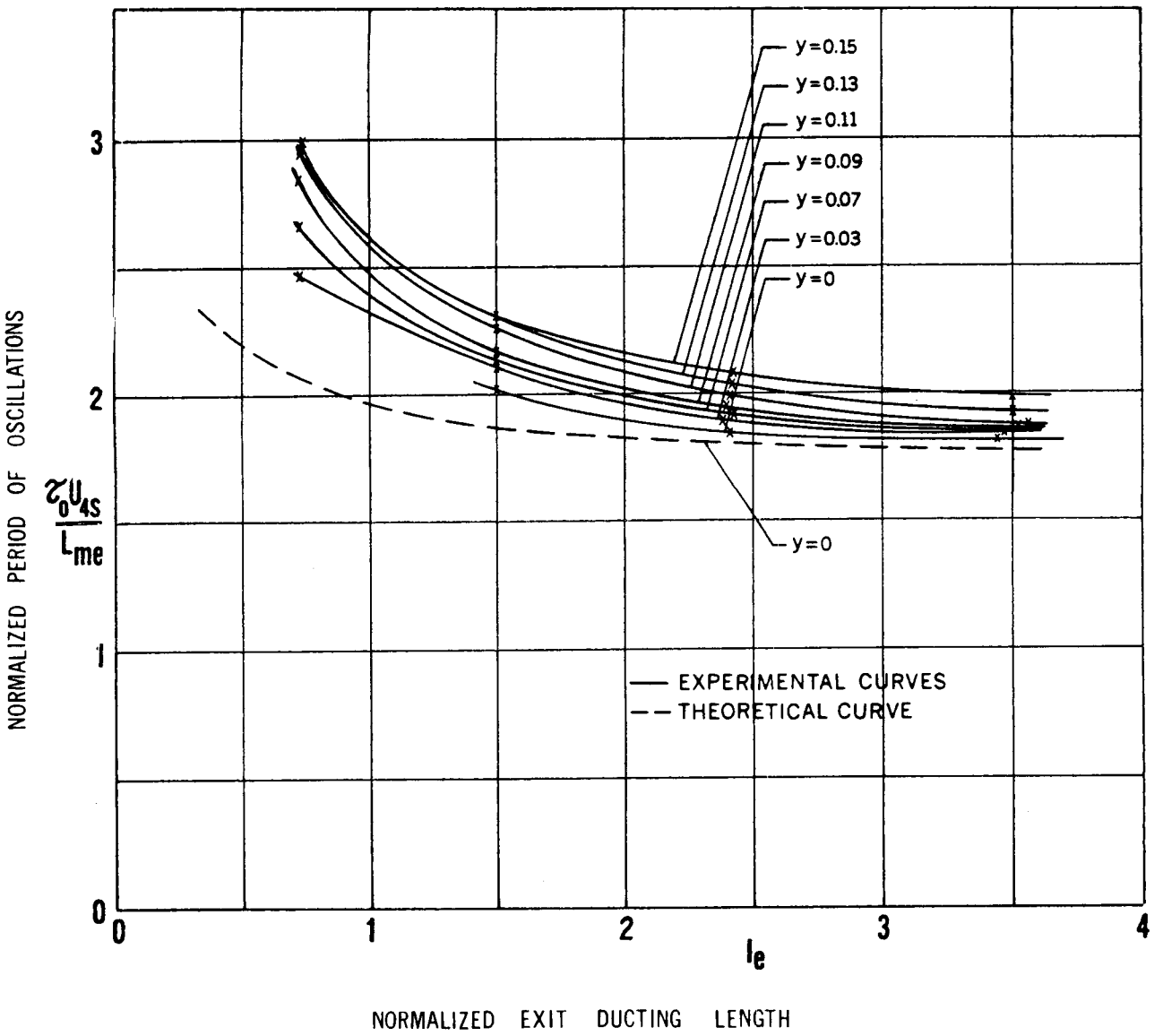

FIG. 39.- TIME PERIOD OF OSCILLATIONS AT STABILITY BOUNDARY